Eur. Phys. J. C (2023) 83:571
https://doi.org/10.1140/epjc/s10052-023-11581-0

THE EUROPEAN PHYSICAL JOURNAL C

Regular Article - Experimental Physics

Search for light Higgs bosons from supersymmetric cascade decays in pp collisions at $\sqrt{s} = 13\,\mathrm{TeV}$

CMS Collaboration*

CERN, 1211 Geneva 23, Switzerland

Received: 28 April 2022 / Accepted: 1 July 2022 / Published online: 6 July 2023

Abstract A search is reported for pairs of light Higgs bosons (H_1) produced in supersymmetric cascade decays in final states with small missing transverse momentum. A data set of LHC pp collisions collected with the CMS detector at $\sqrt{s} = 13\,\mathrm{TeV}$ and corresponding to an integrated luminosity of $138\,\mathrm{fb}^{-1}$ is used. The search targets events where both H_1 bosons decay into $\mathrm{b\bar{b}}$ pairs that are reconstructed as large-radius jets using substructure techniques. No evidence is found for an excess of events beyond the background expectations of the standard model (SM). Results from the search are interpreted in the next-to-minimal supersymmetric extension of the SM, where a "singlino" of small mass leads to squark and gluino cascade decays that can predominantly end in a highly Lorentz-boosted singlet-like H_1 and a singlino-like neutralino of small transverse momentum. Upper limits are set on the product of the squark or gluino pair production cross section and the square of the $\mathrm{b\bar{b}}$ branching fraction of the H_1 in a benchmark model containing almost mass-degenerate gluinos and light-flavour squarks. Under the assumption of an SM-like $\mathrm{H}_1 \to \mathrm{b\bar{b}}$ branching fraction, H_1 bosons with masses in the range 40–120 GeV arising from the decays of squarks or gluinos with a mass of 1200–2500 GeV are excluded at 95% confidence level.

1 Introduction

This paper presents a search for pairs of light Higgs bosons (H_1) produced in supersymmetric (SUSY) [1–8] cascade decays in final states with small missing transverse momentum ($p_{\mathrm{T}}^{\mathrm{miss}}$). Such events can arise from the pair production of squarks ($\tilde{\mathrm{q}}$) and gluinos ($\tilde{\mathrm{g}}$) in the next-to-minimal supersymmetric extension of the standard model (SM) [9] when the lightest SUSY particle (LSP) is a singlino-like neutralino ($\tilde{\chi}_{\mathrm{S}}^0$) of small mass [10]. The $\tilde{\chi}_{\mathrm{S}}^0$ mass eigenstate is dominated by the singlino component and has only small couplings to other SUSY particles, suppressing direct squark or gluino decays to the $\tilde{\chi}_{\mathrm{S}}^0$. Squarks and gluinos decay via the next-to-LSP $\tilde{\chi}_2^0$ into a $\tilde{\chi}_{\mathrm{S}}^0$ and a Higgs, Z, or W boson [10,11]. The case of a singlet-like CP-even H_1, shown in Fig. 1, is the focus of this search. When the $\tilde{\chi}_{\mathrm{S}}^0$ has a far smaller mass than the H_1 and the phase space for the decay $\tilde{\chi}_2^0 \to \mathrm{H}_1 + \tilde{\chi}_{\mathrm{S}}^0$ is small, the H_1 carries much larger momentum than the $\tilde{\chi}_{\mathrm{S}}^0$. In such $p_{\mathrm{T}}^{\mathrm{miss}}$-suppressed scenarios, the key signature for the pair production of squarks and gluinos is a pair of Lorentz-boosted H_1 bosons.

This search targets events with two highly boosted H_1 bosons that decay into $\mathrm{b\bar{b}}$ pairs that are reconstructed as large-radius jets using substructure techniques. This is the first search at the LHC to focus on this type of event, where particles invisible to the detector have only small transverse momentum (p_{T}) and therefore the events are not selected by searches requiring significant $p_{\mathrm{T}}^{\mathrm{miss}}$ [10,12]. Previous searches by the ATLAS and CMS experiments with similar final states have considered events with two boosted SM Higgs bosons and large values of $p_{\mathrm{T}}^{\mathrm{miss}}$ [13,14], or two SM Higgs bosons in resolved final states where each of the four b quarks is reconstructed as a separate jet, with either small [15] or large [14–17] values of $p_{\mathrm{T}}^{\mathrm{miss}}$. This search uses data from

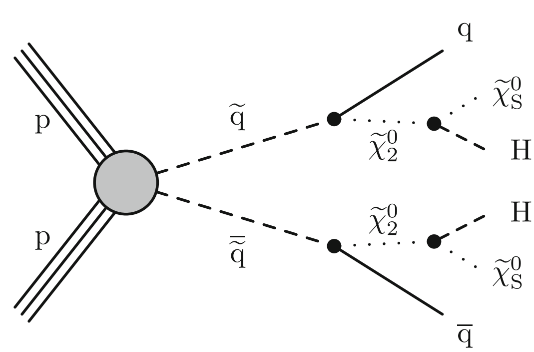

Fig. 1 Diagram of squark pair production and subsequent cascade decay in the benchmark signal model. The particle $\tilde{\chi}_2^0$ is the next-to-LSP, $\tilde{\chi}_{\mathrm{S}}^0$ is the singlino-like LSP, and H_1 is the CP-even singlet-like Higgs boson

* e-mail: cms-publication-committee-chair@cern.ch

pp collisions collected by the CMS detector at $\sqrt{s} = 13$ TeV during 2016–2018, corresponding to an integrated luminosity of 138 fb^{-1} [18–20].

2 Benchmark signal model

A benchmark signal model is established following the work of Ellwanger and Teixeira [10,11]. The eight first- and second-generation squarks are assumed mass-degenerate at the mass m_{SUSY}, and the gluino mass is set at 1% larger. The small gluino-squark mass gap means that the kinematics of the final-state particles are very similar in the $\tilde{q}\tilde{q}$, $\tilde{q}\tilde{g}$, and $\tilde{g}\tilde{g}$ production modes, as little momentum is transferred to the quark in the $\tilde{g} \to \tilde{q} + q$ decay. All SUSY particles other than gluinos and those shown in Fig. 1 are assumed decoupled.

This search targets squarks and gluinos with $m_{\mathrm{SUSY}} > 1200$ GeV. Less massive squarks and gluinos can be probed by $p_{\mathrm{T}}^{\mathrm{miss}}$-based searches, owing to their larger pair-production cross sections [12]. Smaller m_{SUSY} values can also lead to smaller p_{T} of the $\mathrm{H_1}$ than is necessary for the $\mathrm{b\bar{b}}$ pair to be merged in a single jet. The cross sections (σ) for the signal probed in this search, calculated at next-to-leading order (NLO) accuracy in the strong coupling constant (α_{S}) including approximate next-to-NLO (NNLO) corrections and next-to-next-to-leading logarithmic (NNLL) soft gluon corrections [21–29], are shown in Table 1.

The values considered of the $\mathrm{H_1}$ mass ($m_{\mathrm{H_1}}$) and the corresponding $\mathrm{H_1} \to \mathrm{b\bar{b}}$ branching fractions ($\mathcal{B}$) are shown in Table 2. Only events where both $\mathrm{H_1}$ bosons decay into $\mathrm{b\bar{b}}$ pairs are used as signal. The $\mathcal{B}$ values are chosen to be those of an SM-like Higgs boson ($\mathrm{H_{SM}}$) of the corresponding mass [10], as calculated using HDECAY 6.61 [30,31]. The $\mathcal{B}$ values decrease for larger $\mathrm{H_1}$ masses as the virtual WW* and ZZ* decay channels, both of which have sizeable leptonic branching fractions, become more accessible. The region $m_{\mathrm{H_1}} < m_{\mathrm{Z}}$ is therefore where the $p_{\mathrm{T}}^{\mathrm{miss}}$-suppressed all-jet signature is of greatest experimental importance. Nevertheless, to preserve generality, this search attempts to probe as much of the region $m_{\mathrm{H_1}} < 125$ GeV as possible.

Table 1 Inclusive pair-production cross sections calculated at approximately NNLO and NNLL in α_{S} [21–29] for squark mass m_{SUSY} and gluino mass 1% larger. The quoted uncertainty is obtained from variations in the choice of scales, parton distribution functions, and α_{S}

m_{SUSY} (GeV)	$\sigma(\mathrm{pp} \to \tilde{q}\tilde{q}, \tilde{q}\tilde{g}, \tilde{g}\tilde{g})$ [fb]	Uncertainty (%)
1200	580	8
1600	69	9
2000	10	11
2200	4.1	13
2400	1.6	14
2600	0.67	16
2800	0.27	18

In addition to $m_{\mathrm{H_1}}$ and m_{SUSY}, there are two other unknown masses in the benchmark model: those of the $\tilde{\chi}^0_{\mathrm{S}}$ and the $\tilde{\chi}^0_2$. The corresponding degrees of freedom are parameterised by $R_m \equiv m_{\mathrm{H_1}}/m_{\tilde{\chi}^0_2}$ and $\Delta_m \equiv m_{\tilde{\chi}^0_2} - m_{\mathrm{H_1}} - m_{\tilde{\chi}^0_{\mathrm{S}}}$. The $p_{\mathrm{T}}^{\mathrm{miss}}$-suppressed signature arises for values of R_m close to unity, provided $\Delta_m > 0$ to permit the $\tilde{\chi}^0_2 \to \mathrm{H_1} + \tilde{\chi}^0_{\mathrm{S}}$ decay. In this case, the phase space for the $\tilde{\chi}^0_2$decay is small and the $\tilde{\chi}^0_{\mathrm{S}}$ has much smaller mass than the $\mathrm{H_1}$, so the $\tilde{\chi}^0_{\mathrm{S}}$ always carries much less momentum than the $\mathrm{H_1}$. The $p_{\mathrm{T}}^{\mathrm{miss}}$-suppressed signature probed in this search is representative of a significant part of the model parameter space since the momenta of reconstructed objects do not exhibit a strong dependence on R_m and Δ_m in the region $R_m > 0.9$. Models with smaller R_m can be probed by $p_{\mathrm{T}}^{\mathrm{miss}}$-based searches [10,12]. For the benchmark model, the values $R_m = 0.99$ and $\Delta_m = 0.1$ GeV are assumed.

Branching fractions of unity are assumed for the decays $\tilde{q} \to q + \tilde{\chi}^0_2$ and $\tilde{\chi}^0_2 \to \mathrm{H_1} + \tilde{\chi}^0_{\mathrm{S}}$. In the R_m and Δ_m region of the benchmark model, this is true except where $m_{\tilde{\chi}^0_2} > m_{\mathrm{Z}} + m_{\tilde{\chi}^0_{\mathrm{S}}}$. In that case, the $\tilde{\chi}^0_2 \to \mathrm{Z} + \tilde{\chi}^0_{\mathrm{S}}$ decay is permitted if the $\tilde{\chi}^0_2$ has a higgsino component [11]. However, the $\tilde{\chi}^0_2$ is expected to be mainly bino-like for relevant values of its mass [10]. For configurations where the $\mathrm{H_1}$ mass is close to that of the $\mathrm{H_{SM}}$, the decay $\tilde{\chi}^0_2 \to \mathrm{H_{SM}} + \tilde{\chi}^0_{\mathrm{S}}$ is also possible. The signatures for such $\mathrm{H_1}$ and $\mathrm{H_{SM}}$ bosons are indistinguishable in this search. The assumption that the branching fraction for $\tilde{\chi}^0_2 \to \mathrm{H_1} + \tilde{\chi}^0_{\mathrm{S}}$ decay is 100% can therefore be relaxed to the assumption that the branching fractions to $\mathrm{H_1}$ and $\mathrm{H_{SM}}$ sum to unity.

3 The CMS detector

The central feature of the CMS apparatus is a superconducting solenoid of 6 m internal diameter, providing a magnetic field of 3.8 T. A silicon pixel and strip tracker, a lead tungstate crystal electromagnetic calorimeter, and a brass and scintillator hadron calorimeter, each composed of a barrel and two endcap sections, reside within the solenoid volume. Forward calorimeters extend the pseudorapidity (η) coverage provided by the barrel and endcap detectors. Muons are measured in gas-ionisation detectors embedded in the steel flux-return yoke outside the solenoid. Events of interest are selected using a two-tiered trigger system. The first level, composed of custom hardware processors, uses information from the calorimeters and muon detectors to select events at a rate of around 100 kHz within a fixed latency of about 4 μs [32]. The second level, known as the high-level trigger, consists of a farm of processors running a version of the full event reconstruction software optimised

Table 2 The m_{H_1} values in this search and corresponding $H_1 \to b\bar{b}$ branching fractions

m_{H_1} [GeV]	30	35	40	50	60	70	80	90	100	110	120	125
$\mathcal{B}(H_1 \to b\bar{b})$	0.86	0.86	0.86	0.86	0.85	0.84	0.83	0.81	0.79	0.75	0.65	0.58

for fast processing, and reduces the event rate to around 1 kHz before data storage [33]. A more detailed description of the CMS detector, together with a definition of the coordinate system and the kinematic variables, can be found in Ref. [34].

4 Event simulation

The primary background in this search originates from multijet production. Simulated multijet events are used to validate the multijet background estimation based on data (described in Sect. 6), but are not used for any of the final predictions. The remaining significant background is from events with vector bosons that decay into quark–antiquark pairs. Simulated events are used to determine the contributions from $t\bar{t}$, Z+jets, and W+jets production. The expected yields from all other SM sources of background are found to be negligible.

The multijet, Z+jets, and W+jets processes are simulated at leading order (LO) in perturbative quantum chromodynamics (QCD) using MadGraph5_aMC@NLO 2.4.2 [35] with up to four additional partons at the matrix element (ME) level. Simulated signal events for each pair of m_{H_1} and m_{SUSY} values of the benchmark model are generated at LO at the ME level with up to one additional parton using MadGraph5_aMC@NLO 2.3.3. The MLM [36] prescription is used to match partons from the LO ME calculations to those from the parton showers. Simulated $t\bar{t}$ events are produced at NLO in QCD at the ME level with the powheg v2.0 [37–40] generator. The NNPDF2.3, NNPDF3.0, and NNPDF3.1 [41–44] parton distribution functions (PDFs) are used for the signal, 2016 background, and 2017–2018 background simulations, respectively. The parton shower and hadronisation are performed via pythia 8.2 [45]. The CUETP8M1 [46,47] tune is used for the signal and 2016 background simulations, while the CP5 tune [48] is used for the 2017 and 2018 background simulations. The cross section used to normalise the $t\bar{t}$ simulation is calculated at NNLO+NNLL in QCD [49], and those for Z+jets and W+jets are calculated at NNLO in QCD [50–52]. Additional pp interactions within the same or nearby bunch crossings (pileup) are simulated for all events according to the distribution of the number of interactions observed in each bunch crossing [53]. The interactions of particles with the CMS detector are simulated using Geant4 [54].

5 Object reconstruction and event selection

The data are collected using triggers based on the scalar sum of jet p_T (H_T), with a requirement of $H_T > 900$ GeV (2016) and $H_T > 1050$ GeV (2017 and 2018). Events are reconstructed offline using a particle-flow (PF) algorithm [55] that reconstructs and identifies each individual particle (PF candidate) in an event using an optimised combination of information from the components of the CMS detector.

Jets are reconstructed by clustering the PF candidates using the anti-k_T clustering algorithm [56], as implemented in the FastJet package [57]. A distance parameter of 0.4 or 0.8 is used for standard- and large-radius jets, referred to as AK4 and AK8 jets, respectively. The jet momentum is defined as the vectorial sum of all particle momenta in the jet. To mitigate the effect of pileup, constituent charged PF candidates identified to be originating from vertices other than the primary pp interaction vertex are not used in the clustering algorithm. The primary vertex is taken to be the vertex corresponding to the hardest scattering in the event, evaluated using tracking information alone, as described in Section 9.4 of Ref. [58]. For AK4 jets, an offset correction is applied to correct for remaining pileup contributions. For AK8 jets, the pileup-per-particle identification algorithm [59,60] is used to rescale the momenta of constituent neutral particles according to the probability they originated from the primary vertex. This probability is based on a local shape variable that distinguishes between collinear and soft diffuse distributions of the surrounding charged particles that are compatible with the primary vertex. For all jets, jet energy corrections are derived from simulation to bring the measured average response of jets to that of particle-level jets. In situ measurements of the momentum balance in dijet, photon+jet, Z+jet, and multijet events are used to account for any residual differences in jet energy scale and resolution between data and simulation [61,62]. Additional criteria are imposed to reject jets from spurious sources, such as electronics noise and detector malfunctions [63,64].

The identification of AK8 jets originating from two collimated b quarks (double-b tagging) is integral to the reconstruction of the H_1. A discriminant is calculated for each jet using a double-b tagging algorithm that combines tracking and vertexing information in a multivariate approach with no strong dependence on jet mass or p_T [65].

The event preselection requires two AK8 jets with $p_T > 170$ GeV and $|\eta| < 2.4$ (so that they are within the acceptance of the tracker). If there are more than two candidate

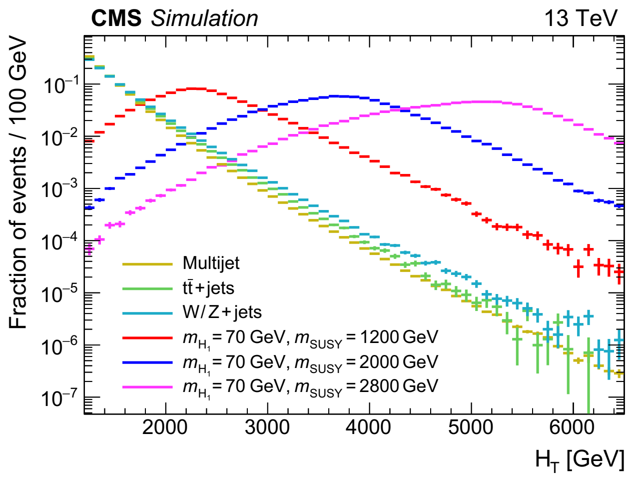

Fig. 2 The H_T distribution in signal events with different values of m_{SUSY}, and in the simulated SM backgrounds, normalised to unit area. The uncertainties are statistical. All events satisfy the preselection

AK8 jets, the two with the largest double-b tag discriminants are selected as most likely to have originated from $H_1 \rightarrow b\bar{b}$ decays. For the offline analysis, $H_T$is defined as the scalar p_T sum of all AK4 jets with $p_T > 40$ GeV and $|\eta| < 3.0$, including AK4 jets with PF candidates clustered into AK8 jets. The H_T distributions for various simulated signal and background processes are shown in Fig. 2, after implementing all preselection requirements. Since the final state contains only jets, the average signal event H_T depends significantly on m_{SUSY}, and signal events with $m_{SUSY} > 1200$ GeV tend to have $H_T > 1500$ GeV.

Additional requirements based on the expected kinematic properties of signal events are applied after the preselection. They define the kinematic event selection:

1. Both selected AK8 jets must have $p_T > 300$ GeV and $|\eta| < 2.4$, characteristic of the jets originating from $H_1 \rightarrow b\bar{b}$ decay in signal events.
2. There must be at least one AK4 jet with $p_T > 300$ GeV and $|\eta| < 3.0$, characteristic of the quarks from squark decays in signal events. Such jets must be separated by $\Delta R \equiv \sqrt{(\Delta\phi)^2 + (\Delta\eta)^2} > 1.4$ from both selected AK8 jets, to avoid being constructed from the same PF candidates.
3. The event H_T must exceed 1500 GeV.

Although the offline H_T resolution is better than that of the trigger-level variable, the offline H_T threshold is comfortably above the trigger-level H_T requirements. The trigger efficiency for this analysis is measured using events collected with a single muon trigger with a muon p_T threshold between 24 and 27 GeV. The efficiency for each data-taking year is nearly 100%. For the 2018 data, the $|\eta|$ selection for the AK4 jets is reduced from 3.0 to 2.4 to avoid a region of the endcap electromagnetic calorimeters affected by large losses in crystal transparency, and therefore increased energy-equivalent electronics noise [66]. This change has a negligible effect on signal acceptance for all considered masses.

The fraction of signal events that satisfy the kinematic selection is essentially independent of m_{H_1}. It increases from about 60 to 80% as m_{SUSY} increases from 1200 to 2000 GeV, after which it remains approximately constant.

5.1 Double-b tag based event selection

The two AK8 jets that are classified as the $H_1 \rightarrow b\bar{b}$ candidates in each event are randomly assigned the labels “A” and “B”. Their double-b tag discriminants define a two-dimensional (2D) parameter space, shown with simulated signal and multijet event distributions in Fig. 3. The signal events are expected to contain two $H_1 \rightarrow b\bar{b}$ decays and therefore accumulate in the region where both double-b tag discriminants are large. The signal-enhanced tag region (TR) is defined as the region where the sum of the two double-b tag discriminants exceeds 1.3, illustrated by the shaded triangle in Fig. 3. Two additional regions are defined in Fig. 3 for use in the multijet background estimation and validation: the control region (CR), a multijet-dominated region with negligible signal; and the validation region (VR), a more signal-like region where one of the two jets has a large double-b tag discriminant. The VR is defined sufficiently far from the TR for the signal contamination to be negligible.

About 50% of the signal events that satisfy the kinematic selection populate the TR, with variation at the level of ±10% across the m_{H_1} and m_{SUSY} parameter space considered. Since the multijet background is dominated by light-flavour quark and gluon initiated jets, only about 3% of these events populate the TR. For the $t\bar{t}$, Z+jets, and W+jets backgrounds, the corresponding figures are 13, 6, and 3%, respectively.

5.2 Soft-drop mass based signal and sideband regions

In signal events, both selected AK8 jets are likely to originate from $H_1 \rightarrow b\bar{b}$ decays and therefore have a jet mass close to m_{H_1}. The multijet background has no resonant mass peak, while the other backgrounds are only expected to exhibit peaks near the known top quark and vector bosons masses, which means that an accurate reconstruction of the jet mass is important in distinguishing signal from background. The AK8 jet masses are evaluated using the “soft-drop” algorithm [67] (with a soft-drop threshold of $z_{cut} = 0.1$ and angular exponent of $\beta = 0$), in which wide-angle soft radiation is removed recursively from a jet. In signal events this algorithm achieves a relative jet mass resolution from 10% for $m_{H_1} = 125$ GeV to 20% for $m_{H_1} = 30$ GeV.

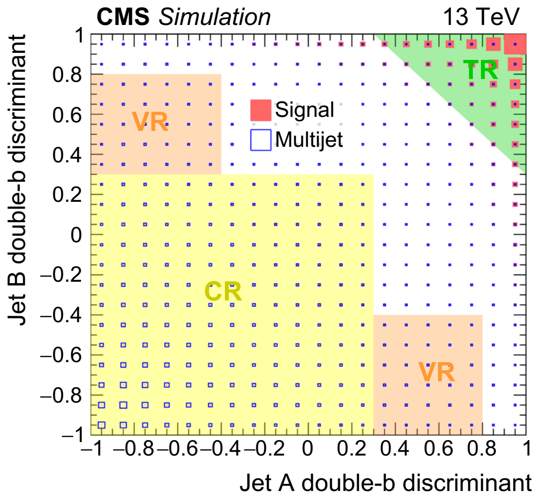

Fig. 3 Distributions of simulated signal and multijet events in the 2D double-b tag discriminant plane, where the fractions of events in each bin are represented by the areas of the filled red and open blue squares, respectively. The signal parameters are $m_{\mathrm{H}_1} = 70\,\mathrm{GeV}$ and $m_{\mathrm{SUSY}} = 2000\,\mathrm{GeV}$. The kinematic selection is implemented with the masses of the two AK8 jets required to be within the set of signal and sideband mass regions defined in Sect. 5.2. The green, yellow, and orange shaded areas represent the tag region (TR), control region (CR), and validation region (VR), respectively. Of the plotted signal events, 65% fall within the TR

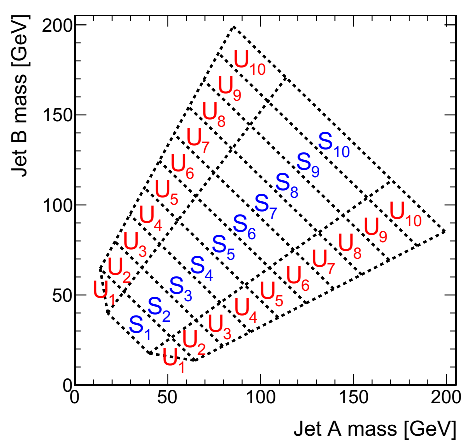

Fig. 4 Map of mass regions used in the 2D soft-drop mass plane. The regions labelled S_i are the signal mass regions, and the disjoint regions U_i form the corresponding sidebands

The soft-drop masses of the two AK8 jets define a 2D parameter space, shown in Fig. 4, in which 10 signal regions (S_i) and 10 sideband regions (U_i) are defined. The S_i contain events in which the two H_1-candidate jets have approximately the same soft-drop mass. The width of each S_i corresponds to about four times the experimental soft-drop mass resolution for the relevant simulated value of m_{H_1}.

The event distributions for a set of signal models with different m_{H_1} values are shown in Fig. 5, with the signal and sideband mass regions overlaid. The peaks in the signal distributions where one or both AK8 jets have a soft-drop mass close to zero result from a selected jet originating from a single parton or one of the $\mathrm{H}_1 \to \mathrm{b\bar{b}}$ decays lying outside the acceptance of the jet reconstruction algorithm. The latter can happen when the angular separation of the b quarks exceeds the AK8 jet distance parameter, or when the ratio of the b quark p_{T} values is larger than 9 (such that the softer b quark would not satisfy the z_{cut} threshold in the soft-drop algorithm). For signal models with $40 < m_{\mathrm{H}_1} < 125\,\mathrm{GeV}$, $\approx$50% of the events that satisfy the kinematic and TR selection fall within any of the S_i. However, for $m_{\mathrm{H}_1} < 35\,\mathrm{GeV}$ the bulk of the distribution is lower in mass than S_1, leading to a rapid decrease in signal acceptance.

The distributions of background events are also shown in Fig. 5. The majority of multijet events contain at least one AK8 jet evaluated to have a small soft-drop mass, reflecting the characteristic one-prong structure of quark and gluon jets. After applying the kinematic and TR selection criteria, approximately 5% of multijet events fall within any of the S_i, with greater probability at small masses. For the vector boson and $\mathrm{t\bar{t}}$ backgrounds the corresponding figures are 7 and 19%, respectively, concentrated in the S_i corresponding to masses between the W boson and top quark masses.

For each S_i there are two corresponding sideband regions, U_i, used for the multijet background estimation described in Sect. 6. The sideband regions U_1 have a triangular form to avoid the region of very small soft-drop masses, where the density from multijet events increases sharply.

5.3 Categorisation in H_{T} and expected yields

The selected events are classified according to three H_{T} categories: 1500–2500, 2500–3500, and above 3500 GeV. Each H_{T} category is divided into the 10 mass signal regions S_i defined in Fig. 4, resulting in a total of 30 search regions for each data-taking year. As can be seen in Fig. 6 for TR data summed over the three data-taking years, the search region yields can be visualised through a 30-bin histogram where bins 1–10 represent the S_i, in ascending order, for the first H_{T} category. The subsequent two sets of 10 bins represent the results for the second and third H_{T} categories. The primary background is from multijet events, estimated from data using the method described in Sect. 6. The expected contribution from $\mathrm{t\bar{t}}$ events is also significant, particularly in the larger soft-drop mass regions populated by jets from hadronic top quark or W boson decays. The $\mathrm{t\bar{t}}$ simulation is validated in a dedicated $\mathrm{t\bar{t}}$-enriched control region in data. In Fig. 4 this is the triangular region of the parameter space with both jet masses below 200 GeV and above the upper boundary of mass region 10. The yields from Z+jets and W+jets production are small in comparison. All expected SM backgrounds tend to exhibit small values of H_{T} compared to signal.

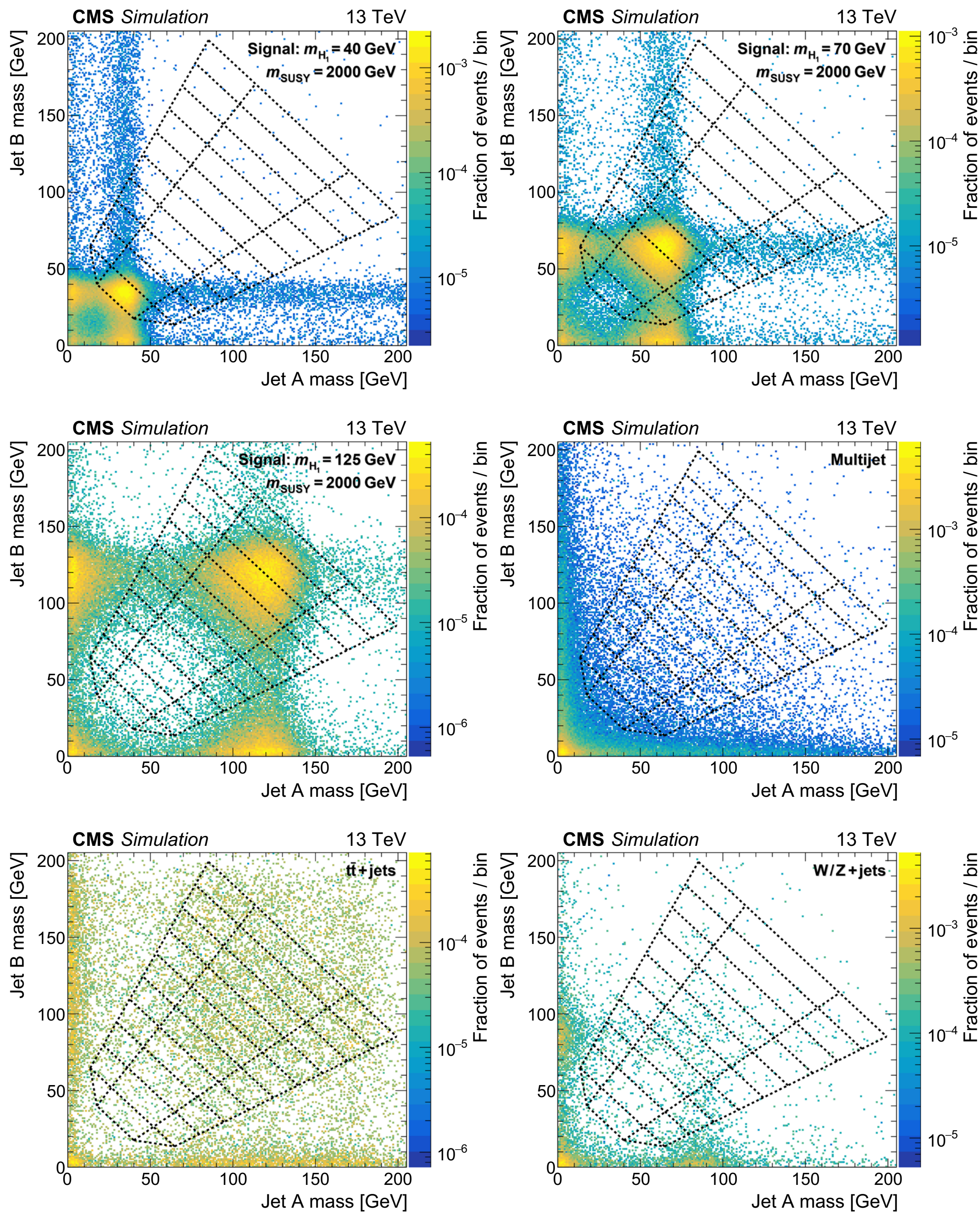

Fig. 5 The normalised distribution of events in the 2D soft-drop mass plane overlaid by the map of mass regions. The upper left, upper right, and middle left panels correspond to signal events for $m_{SUSY} =$ 2000 GeV and m_{H_1} values of 40, 70, and 125 GeV, respectively. The panels at middle right, lower left, and lower right correspond to simulated multijet, $t\bar{t}$, and vector boson backgrounds, respectively. All events satisfy the TR requirement and the kinematic selection

The distributions in signal events for $m_{H_1} = 70$ GeV and $m_{SUSY} = 1200$, 2000 and 2800 GeV are also shown in Fig. 6. Although the production cross section decreases quickly with increasing m_{SUSY}, the fraction of events in the larger-H_T categories increases. Within each H_T category, the distribution of events in the 10 S_i bins is described by a peak with a width of about three bins, centred near the model value of m_{H_1}.

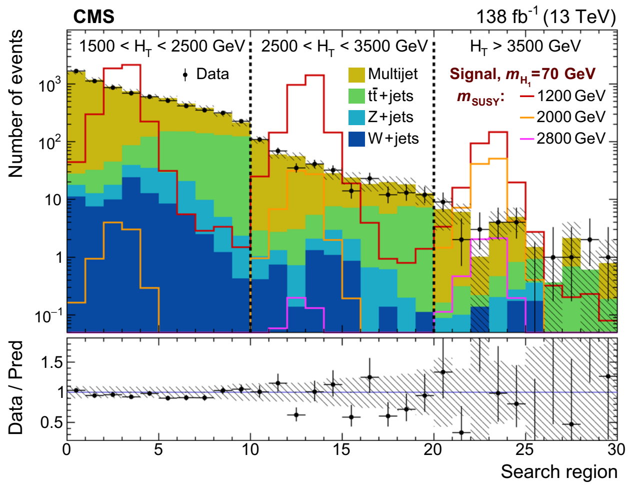

Fig. 6 Observed and expected yields in the TR for each of the 30 search regions, summed over the three data-taking years. The multijet background is estimated from data using the method described in Sect. 6, while the other backgrounds are simulated. Example signal distributions are shown for $m_{\mathrm{H}_1} = 70$ GeV and $m_{\mathrm{SUSY}} = 1200, 2000$, and 2800 GeV. The error bars represent the statistical uncertainties and the hatched bands the systematic uncertainties

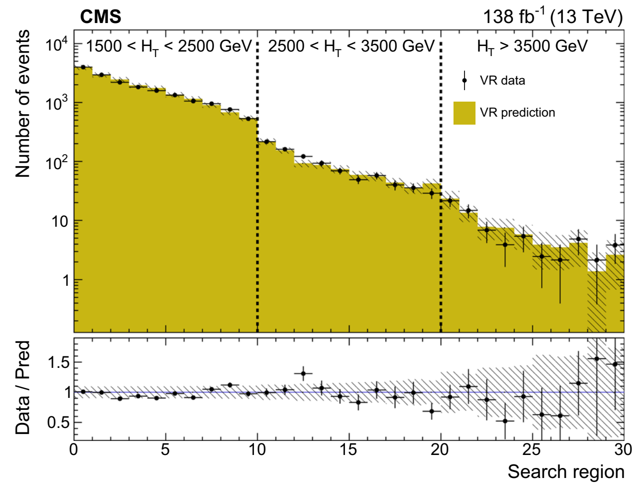

Fig. 7 A comparison of the predicted and observed multijet yields in the validation region (VR), after subtraction of the other simulated backgrounds. The prediction is made separately for the three data-taking years, and the results are summed. The error bars on the data points represent their statistical uncertainties. The uncertainties in the predicted yields (statistical and systematic) are indicated by the hatched bands

6 Multijet background estimation from data

The mass sideband regions U_i form a basis for using data to estimate the multijet background. The density of the multijet background is approximately uniform within each of the 10 mass regions (spanning S_i and U_i for each region i illustrated in Fig. 4). Apart from U_1, each U_i is constructed to have the same area as S_i such that the corresponding multijet yields, respectively denoted $\hat{U}_i$ and $\hat{S}_i$, are approximately equal. The observed ratios of S_i to U_i yields, F_i, are measured in CR data. The F_i factors are found to be close to unity except for the F_1 values which are approximately 1.5.

The multijet background in the TR is estimated independently for each signal region S_i:

$$\hat{S}_i^{\mathrm{TR}} = F_i\, \hat{U}_i^{\mathrm{TR}}, \tag{1}$$

where $\hat{U}_i^{\mathrm{TR}}$ is the observed TR yield in sideband region U_i after subtracting the contributions from the other simulated backgrounds. In rare cases where the prediction $\hat{S}_i^{\mathrm{TR}}$ is negative, it is set equal to zero.

Since the F_i factors are measured and applied in different regions of double-b tag discriminant space, any correlation between the soft-drop mass and the double-b tag discriminant of AK8 jets can bias the prediction of Eq. (1). Using a sample of data satisfying an alternative kinematic event selection with the requirement for one or more AK4 jets inverted, the variation of F_i between the TR and the CR is found to be less than 10%.

The overall accuracy of the multijet estimation is assessed through closure tests. First the method is applied to simulated multijet events in the TR where, within statistical uncertainties, the predicted yields are consistent with the simulated yields for each data-taking year. Second the method is applied in the multijet-dominated VR data (defined in Fig. 3) by making the appropriate modification to Eq. (1): $\hat{S}_i^{\mathrm{VR}} = F_i\, \hat{U}_i^{\mathrm{VR}}$. The resulting predicted and observed VR yields are consistent within uncertainties, as shown in Fig. 7. Based on the results of the closure tests, a systematic uncertainty of 15 (30%) is assigned in the lower two H_{T} categories (upper H_{T} category).

7 Systematic uncertainties

The simulated events for signal and the $\mathrm{t\bar{t}}$, Z+jets, and W+jets backgrounds are affected by various systematic uncertainties. The efficiency for tagging (mistagging) a jet originating from two b quarks (a light-flavour quark or gluon) is corrected to match that observed in data [65]. The uncertainty in this correction corresponds to $\approx 10\%$ in the simulated signal and background yields. The uncertainties related to the jet energy corrections are applied to the jet properties in bins of p_{T} and η. These uncertainties affect the event H_{T}, leading to an $\approx 4\%$ migration of events between adjacent H_{T} categories. The uncertainty in the soft-drop mass scale in simulation relative to data leads to a migration of events between adjacent S_i and U_i regions of up to 10%. The uncertainty in the simulated soft-drop mass resolution affects the widths of the simulated mass peaks. This effect is larger for signal models with small m_{H_1} and can reduce the S_i selection efficiency by up to 20%.

The systematic uncertainties are assumed to be fully correlated among the data-taking years except for the 2016 double-b tagging uncertainties, which are assumed uncorrelated because the CMS pixel detector was upgraded prior to 2017 data-taking. Changing these correlation assumptions is found to have only a small effect on the final results. Systematic uncertainties related to integrated luminosity, pileup, PDFs, renormalisation and factorisation scales, modelling of initial-state radiation, and background cross sections were also evaluated, along with the statistical uncertainties in the simulation, and were found to make negligible contributions to the total uncertainty.

Systematic uncertainties in multijet yields arise from the systematic uncertainties in the F_i factors. As described in Sect. 6, an uncertainty of 15% is applied to the F_i in the lower two H_{T} categories and 30% in the upper H_{T} category, uncorrelated among different F_i. Except in the lowest H_{T} category, the total uncertainty in the multijet yield is dominated by the statistical uncertainty in $\hat{U}_i^{\mathrm{TR}}$.

8 Results

Binned maximum likelihood fits to the data in all 30 search regions S_i for each data-taking year are carried out under background-only and signal+background hypotheses. The corresponding sideband regions U_i are fitted simultaneously, thereby constraining the multijet contributions to the search region yields through Eq. (1). The likelihood functions are defined through the product of 90 × 2 Poisson distributions [68], one for each search region and one for each sideband region, with additional constraint terms for the “nuisance” parameters that account for the systematic uncertainties summarised in Sect. 7. Figure 8 compares the result of the background-only fit to the yields in the search regions for the combination of 2016, 2017, and 2018 data. There is no evidence for deviations of the data from the fitted background. The values and uncertainties of most nuisance parameters are unchanged in the fit, but the ones corresponding to the F_i are constrained through Eq. (1) when the yields $\hat{S}_i^{\mathrm{TR}}$ and $\hat{U}_i^{\mathrm{TR}}$ are sufficiently large.

Signal+background fits are used to set 95% confidence level (CL) upper limits on the product $\sigma\mathcal{B}^2$ for the mass points in the benchmark signal model. The limits are set using the modified frequentist CL_s criterion [69,70], with the profile likelihood ratio as test statistic [68]. The observed and expected 95% CLupper limits on $\sigma\mathcal{B}^2$ are shown in Fig. 9, as functions of m_{H_1} for constant m_{SUSY}. The upper limits are weaker for models with $m_{\mathrm{H}_1} < 35\,\mathrm{GeV}$, for which the signal-event distribution in the 2D soft-drop mass plane peaks outside the signal regions. The limits have no significant dependence on m_{SUSY} for models with $m_{\mathrm{SUSY}} > 2000\,\mathrm{GeV}$, whose signal events mostly populate the upper H_{T} category (as shown in Fig. 6).

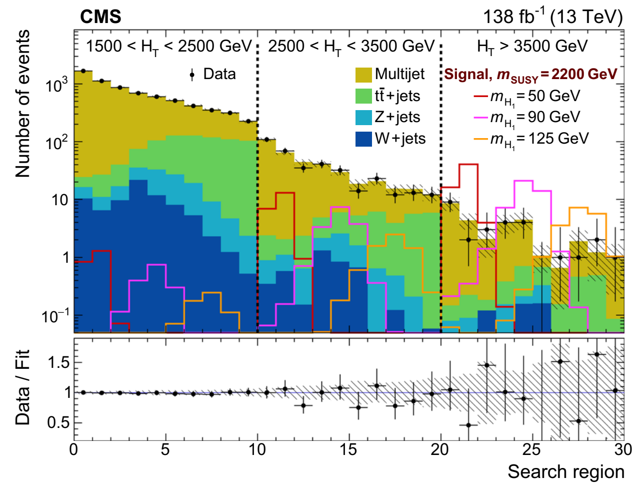

Fig. 8 Yields in all search regions after the background-only fit, summed over the three data-taking years. Example signal contributions used in the signal+background fits are shown for $m_{\mathrm{SUSY}} = 2200\,\mathrm{GeV}$, and $m_{\mathrm{H}_1} = 50$, 90, and 125 GeV. The error bars represent the statistical uncertainties and the hatched bands the systematic uncertainties

The $\sigma\mathcal{B}^2$ upper limits are used in conjunction with the theoretical σ and $\mathcal{B}$ values from Sect. 2 to exclude ranges of masses in m_{H_1} and m_{SUSY} in the benchmark model. The observed 95% CLupper limits on r, the ratio of measured and theoretical values of $\sigma\mathcal{B}^2$, are shown in Fig. 10, with the corresponding exclusion contours at $r = 1$. Masses $1200 < m_{\mathrm{SUSY}} < 2500\,\mathrm{GeV}$ are excluded within the range $40 < m_{\mathrm{H}_1} < 120\,\mathrm{GeV}$. Expected exclusion contours for the background-only scenario agree within one standard deviation with the observed contours. In the region $110 < m_{\mathrm{H}_1} < 125\,\mathrm{GeV}$, $\mathcal{B}$ starts to decrease more quickly (as shown in Table 2), leading to a corresponding reduction in sensitivity. Most of the sensitivity at large m_{SUSY} comes from the $H_{\mathrm{T}} > 3500\,\mathrm{GeV}$ region, where the statistical uncertainties in the observed yields are dominant over systematic uncertainties. This search does not explore the region outside of that shown in Fig. 10.

To aid reinterpretation of the search by reducing the model-dependence, limits evaluated using only the upper H_{T} category are presented in Appendix A. Tabulated results are provided in the HEPData record for this analysis [71].

9 Summary

This paper presents a search for pairs of light Higgs bosons (H_1) produced in supersymmetric cascade decays. The targeted final states have small amounts of missing transverse momentum and two $\mathrm{H}_1 \to \mathrm{b}\bar{\mathrm{b}}$ decays that are reconstructed

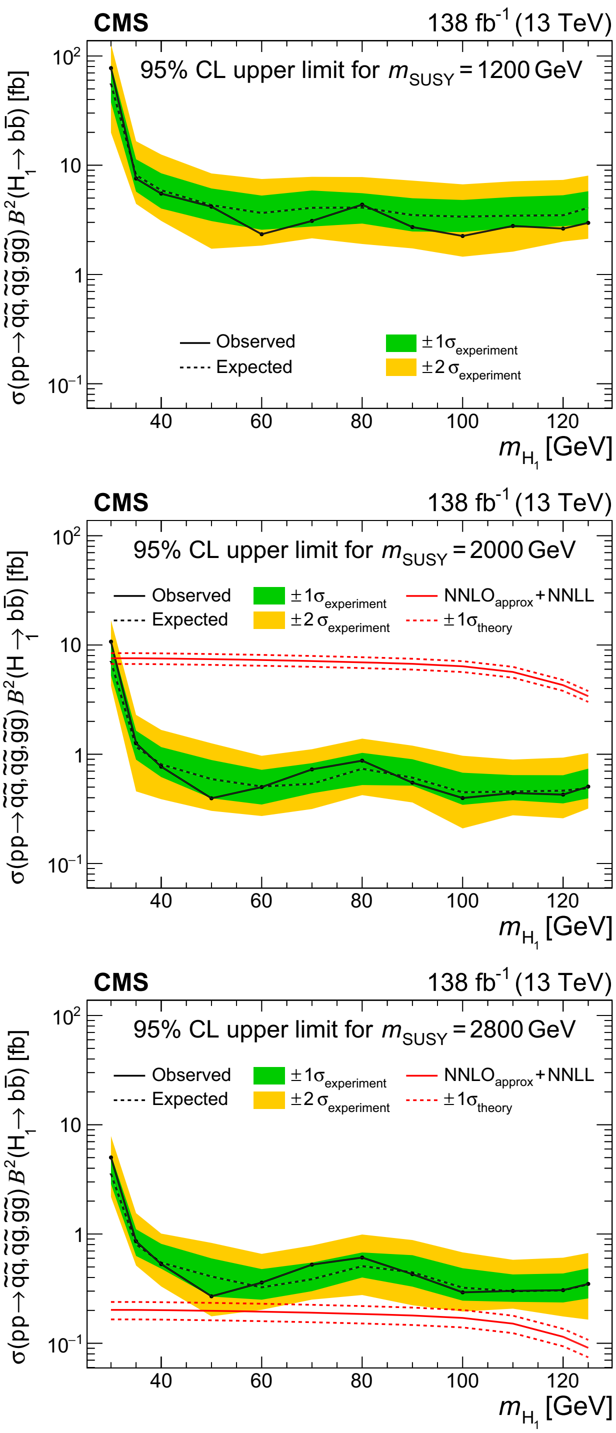

Fig. 9 Upper limits at 95% CL on $\sigma\mathcal{B}^2$ as a function of m_{H_1}, for m_{SUSY} values of 1200 (upper), 2000 (middle), and 2800 GeV (lower). The solid and dashed black lines indicate the observed and median expected limits, respectively. The inner (green) band and the outer (yellow) band indicate the regions containing 68 and 95%, respectively, of the distribution of limits expected under the background-only hypothesis. The solid and dashed red lines show the theoretical value of $\sigma\mathcal{B}^2$ and its uncertainty [21–30]. In the upper plot, these $\sigma\mathcal{B}^2$ values are beyond the maximum of the vertical axis

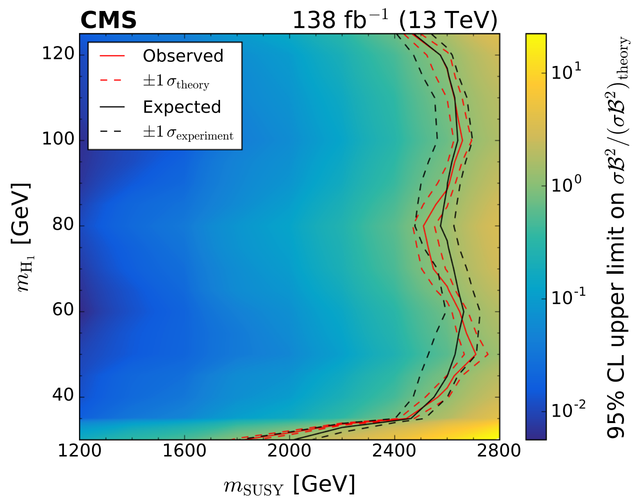

Fig. 10 The observed 95% CL upper limit on $\sigma\mathcal{B}^2/(\sigma\mathcal{B}^2)_{theory}$, quantified by the colour scale as a function of m_{H_1} and m_{SUSY}. The solid and dashed red lines indicate the observed excluded region and its theoretical uncertainty, respectively. The solid and dashed black lines respectively represent the expected excluded region and its 68% CL interval, under the background-only hypothesis

as large-radius jets using substructure techniques. The search is based on data from pp collisions collected by the CMS experiment at $\sqrt{s} = 13$ TeV during 2016–2018, corresponding to an integrated luminosity of 138 fb^{-1}.

With no evidence found for an excess of events beyond the background expectations of the standard model (SM), the results are interpreted in the next-to-minimal supersymmetric extension of the SM (NMSSM), where a "singlino" of small mass leads to squark and gluino cascade decays that can predominantly end in a highly Lorentz-boosted singlet-like H_1 and a singlino-like neutralino of small transverse momentum.

Upper limits are set on the product of the production cross section and the square of the $b\bar{b}$ branching fraction of the H_1 for an NMSSM benchmark model with almost mass-degenerate gluinos and light-flavour squarks and branching fractions of unity for the cascade decays ending with the H_1. Under the assumption of an SM-like $H_1 \to b\bar{b}$ branching fraction, H_1 bosons with masses in the range 40–120 GeV arising from the decays of squarks or gluinos with a mass of 1200 to 2500 GeV are excluded at 95% confidence level.

Data Availability Statements This manuscript has no associated data or the data will not be deposited. [Authors' comment: Release and preservation of data used by the CMS Collaboration as the basis for publications is guided by the CMS policy as stated in https://cms-docdb.cern.ch/cgi-bin/PublicDocDB/RetrieveFile?docid =6032\&filename=CMSDataPolicyV1.2.pdf\&version=2 CMSdatapreservation,re-useandopenaccesspolicy.]

Declarations

Conflict of interest The authors declare that they have no conflict of interest.

Funded by SCOAP[3]. SCOAP[3] supports the goals of the International Year of Basic Sciences for Sustainable Development.

A Simplified analysis for reinterpretation

To aid reinterpretation of the search, a simplified analysis is performed using only the 10 search regions in the upper H_T category. The value A_{kin} is defined as the product of acceptance and efficiency for a signal event to satisfy the kinematic selection (defined in Sect. 5) and the $H_T > 3500$ GeV requirement. The value of A_{kin} is common among all 10 search regions in the simplified analysis, and is quoted for the benchmark signal model in Table 3. Upper limits on the product $\sigma \mathcal{B}^2 A_{kin}$ as a function of m_{H_1} are set in Fig. 11, from which $\sigma \mathcal{B}^2$ limits for different signal models can be derived through division by the appropriate value of A_{kin}. Since the upper H_T category provides most of the sensitivity for $m_{SUSY} > 2000$ GeV in the nominal analysis, the $\sigma \mathcal{B}^2$ upper limits in this region are not much weaker in the simplified analysis. This is not the case in the region $m_{SUSY} < 2000$ GeV, where the lower H_T categories become important.

The double-b tag and mass region selections are not considered in A_{kin}. This is done for simplicity, and because the fraction of events satisfying these selections is not found to be strongly model-dependent (except for the dependence on m_{H_1}, which is accounted for explicitly in Fig. 11). For the benchmark model, this fraction is found to be independent of m_{SUSY} within 10% in the region $1600 < m_{SUSY} < 2800$ GeV and $35 < m_{H_1} < 125$ GeV. This approximate independence does not hold for models with $m_{SUSY} < 1600$ GeV, where the H_1 p_T distribution has substantial contributions below the p_T necessary for the $H_1 \rightarrow b\bar{b}$ decay products to be merged in a single AK8 jet. Only models with typical $b\bar{b}$ angular separation $\Delta R < 0.8$ should be considered for reinterpretation.

Table 3 Reference values of the product of kinematic acceptance and efficiency (A_{kin}) for the $H_T > 3500$ GeV region for the benchmark signal model with different values of m_{SUSY}. These values are independent of m_{H_1} within 2% in the range $30 < m_{H_1} < 125$ GeV

m_{SUSY} [GeV]	1600	2000	2200	2400	2600	2800
A_{kin}	0.17	0.46	0.58	0.66	0.71	0.74

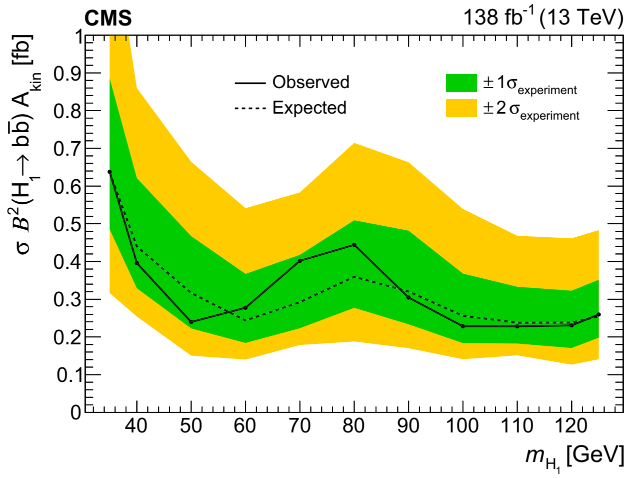

Fig. 11 The observed and expected 95% CL upper limit on the product of $\sigma \mathcal{B}^2$ and A_{kin}, the kinematic acceptance and efficiency for the $H_T > 3500$ GeV region, as a function of m_{H_1}. The results are independent of m_{SUSY} within 10% in the range $1600 < m_{SUSY} < 2800$ GeV. The solid and dashed black lines indicate the observed and median expected limits, respectively. The inner (green) band and the outer (yellow) band indicate the regions containing 68 and 95%, respectively, of the distribution of limits expected under the background-only hypothesis

References

1. P. Ramond, Dual theory for free fermions. Phys. Rev. D **3**, 2415 (1971). https://doi.org/10.1103/PhysRevD.3.2415
2. Y.A. Golfand, E.P. Likhtman, Extension of the algebra of Poincaré group generators and violation of P invariance. JETP Lett. **13**, 323 (1971). http://jetpletters.ru/ps/1584/article_24309.pdf
3. A. Neveu, J.H. Schwarz, Factorizable dual model of pions. Nucl. Phys. B **31**, 86 (1971). https://doi.org/10.1016/0550-3213(71)90448-2
4. D.V. Volkov, V.P. Akulov, Possible universal neutrino interaction. JETP Lett. **16**, 438 (1972). http://www.jetpletters.ru/ps/1766/article_26864.pdf
5. J. Wess, B. Zumino, A Lagrangian model invariant under supergauge transformations. Phys. Lett. B **49**, 52 (1974). https://doi.org/10.1016/0370-2693(74)90578-4
6. J. Wess, B. Zumino, Supergauge transformations in four dimensions. Nucl. Phys. B **70**, 39 (1974). https://doi.org/10.1016/0550-3213(74)90355-1
7. P. Fayet, Supergauge invariant extension of the Higgs mechanism and a model for the electron and its neutrino. Nucl. Phys. B **90**, 104 (1975). https://doi.org/10.1016/0550-3213(75)90636-7

8. H.P. Nilles, Supersymmetry, supergravity and particle physics. Phys. Rep. **110**, 1 (1984). https://doi.org/10.1016/0370-1573(84)90008-5
9. U. Ellwanger, C. Hugonie, A.M. Teixeira, The next-to-minimal supersymmetric standard model. Phys. Rep. **496**, 1 (2010). https://doi.org/10.1016/j.physrep.2010.07.001. arXiv:0910.1785
10. U. Ellwanger, A. Teixeira, NMSSM with a singlino LSP: possible challenges for searches for supersymmetry at the LHC. JHEP **10**, 113 (2014). https://doi.org/10.1007/JHEP10(2014)113. arXiv:1406.7221
11. U. Ellwanger, A. Teixeira, Excessive Higgs pair production with little MET from squarks and gluinos in the NMSSM. JHEP **04**, 172 (2015). https://doi.org/10.1007/JHEP04(2015)172. arXiv:1412.6394
12. A. Titterton et al., Exploring sensitivity to NMSSM signatures with low missing transverse energy at the LHC. JHEP **10**, 064 (2018). https://doi.org/10.1007/JHEP10(2018)064. arXiv:1807.10672
13. CMS Collaboration, Search for physics beyond the standard model in events with high-momentum Higgs bosons and missing transverse momentum in proton-proton collisions at 13 TeV. Phys. Rev. Lett. **120**, 241801 (2018). https://doi.org/10.1103/PhysRevLett.120.241801. arXiv:1712.08501
14. CMS Collaboration, Search for higgsinos decaying to two Higgs bosons and missing transverse momentum in proton-proton collisions at $\sqrt{s} = 13$ TeV. JHEP **05**, 014 (2022). https://doi.org/10.1007/JHEP05(2022)014. arXiv:2201.04206
15. ATLAS Collaboration, Search for pair production of higgsinos in final states with at least three b-tagged jets in $\sqrt{s} = 13$ TeV pp collisions using the ATLAS detector. Phys. Rev. D **98**, 092002 (2018). https://doi.org/10.1103/PhysRevD.98.092002. arXiv:1806.04030
16. CMS Collaboration, Searches for electroweak neutralino and chargino production in channels with Higgs, Z, and W bosons in pp collisions at 8 TeV. Phys. Rev. D **90**, 092007 (2014). https://doi.org/10.1103/PhysRevD.90.092007. arXiv:1409.3168
17. CMS Collaboration, Search for higgsino pair production in pp collisions at $\sqrt{s} = 13$ TeV in final states with large missing transverse momentum and two Higgs bosons decaying via $\mathrm{H} \to \mathrm{b\bar{b}}$. Phys. Rev. D **97**, 032007 (2018). https://doi.org/10.1103/PhysRevD.97.032007. arXiv:1709.04896
18. CMS Collaboration, Precision luminosity measurement in proton-proton collisions at $\sqrt{s} = 13$ TeV in 2015 and 2016 at CMS. Eur. Phys. J. C **81**, 800 (2021). https://doi.org/10.1140/epjc/s10052-021-09538-2. arXiv:2104.01927
19. CMS Collaboration, CMS luminosity measurement for the 2017 data-taking period at $\sqrt{s} = 13$ TeV, CMS Physics Analysis Summary CMS-PAS-LUM-17-004 (2018). https://cds.cern.ch/record/2621960
20. CMS Collaboration, CMS luminosity measurement for the 2018 data-taking period at $\sqrt{s} = 13$ TeV, CMS Physics Analysis Summary CMS-PAS-LUM-18-002 (2019). https://cds.cern.ch/record/2676164
21. W. Beenakker, R. Höpker, M. Spira, P.M. Zerwas, Squark and gluino production at hadron colliders. Nucl. Phys. B **492**, 51 (1997). https://doi.org/10.1016/S0550-3213(97)00084-9. arXiv:hep-ph/9610490
22. A. Kulesza, L. Motyka, Threshold resummation for squark–antisquark and gluino-pair production at the LHC. Phys. Rev. Lett. **102**, 111802 (2009). https://doi.org/10.1103/PhysRevLett.102.111802. arXiv:0807.2405
23. A. Kulesza, L. Motyka, Soft gluon resummation for the production of gluino–gluino and squark–antisquark pairs at the LHC. Phys. Rev. D **80**, 095004 (2009). https://doi.org/10.1103/PhysRevD.80.095004. arXiv:0905.4749
24. W. Beenakker et al., Soft-gluon resummation for squark and gluino hadroproduction. JHEP **12**, 041 (2009). https://doi.org/10.1088/1126-6708/2009/12/041. arXiv:0909.4418
25. W. Beenakker et al., Squark and gluino hadroproduction. Int. J. Mod. Phys. A **26**, 2637 (2011). https://doi.org/10.1142/S0217751X11053560. arXiv:1105.1110
26. W. Beenakker et al., NNLL resummation for squark–antisquark pair production at the LHC. JHEP **01**, 076 (2012). https://doi.org/10.1007/JHEP01(2012)076. arXiv:1110.2446
27. W. Beenakker et al., Towards NNLL resummation: hard matching coefficients for squark and gluino hadroproduction. JHEP **10**, 120 (2013). https://doi.org/10.1007/JHEP10(2013)120. arXiv:1304.6354
28. W. Beenakker et al., NNLL resummation for squark and gluino production at the LHC. JHEP **12**, 023 (2014). https://doi.org/10.1007/JHEP12(2014)023. arXiv:1404.3134
29. W. Beenakker et al., NNLL-fast: predictions for coloured supersymmetric particle production at the LHC with threshold and Coulomb resummation. JHEP **12**, 133 (2016). https://doi.org/10.1007/JHEP12(2016)133. arXiv:1607.07741
30. A. Djouadi, J. Kalinowski, M. Spira, HDECAY: a program for Higgs boson decays in the standard model and its supersymmetric extension. Comput. Phys. Commun. **108**, 56 (1998). https://doi.org/10.1016/S0010-4655(97)00123-9. arXiv:hep-ph/9704448
31. A. Djouadi, J. Kalinowski, M. Mühlleitner, M. Spira, HDECAY: twenty++ years after. Comput. Phys. Commun. **238**, 214 (2019). https://doi.org/10.1016/j.cpc.2018.12.010. arXiv:1801.09506
32. CMS Collaboration, Performance of the CMS Level-1 trigger in proton–proton collisions at $\sqrt{s} = 13$ TeV. JINST **15**, P10017 (2020). https://doi.org/10.1088/1748-0221/15/10/P10017. arXiv:2006.10165
33. CMS Collaboration, The CMS trigger system. JINST **12**, P01020 (2017). https://doi.org/10.1088/1748-0221/12/01/P01020. arXiv:1609.02366
34. CMS Collaboration, The CMS experiment at the CERN LHC. JINST **3**, S08004 (2008). https://doi.org/10.1088/1748-0221/3/08/S08004
35. J. Alwall et al., The automated computation of tree-level and next-to-leading order differential cross sections, and their matching to parton shower simulations. JHEP **07**, 079 (2014). https://doi.org/10.1007/JHEP07(2014)079. arXiv:1405.0301
36. J. Alwall et al., Comparative study of various algorithms for the merging of parton showers and matrix elements in hadronic collisions. Eur. Phys. J. C **53**, 473 (2008). https://doi.org/10.1140/epjc/s10052-007-0490-5. arXiv:0706.2569
37. S. Frixione, P. Nason, G. Ridolfi, A positive-weight next-to-leading-order Monte Carlo for heavy flavour hadroproduction. JHEP **09**, 126 (2007). https://doi.org/10.1088/1126-6708/2007/09/126. arXiv:0707.3088
38. P. Nason, A new method for combining NLO QCD with shower Monte Carlo algorithms. JHEP **11**, 040 (2004). https://doi.org/10.1088/1126-6708/2004/11/040. arXiv:hep-ph/0409146
39. S. Frixione, P. Nason, C. Oleari, Matching NLO QCD computations with parton shower simulations: the POWHEG method. JHEP **11**, 070 (2007). https://doi.org/10.1088/1126-6708/2007/11/070. arXiv:0709.2092
40. S. Alioli, P. Nason, C. Oleari, E. Re, A general framework for implementing NLO calculations in shower Monte Carlo programs: the POWHEG BOX. JHEP **06**, 043 (2010). https://doi.org/10.1007/JHEP06(2010)043. arXiv:1002.2581
41. NNPDF Collaboration, Unbiased global determination of parton distributions and their uncertainties at NNLO and LO. Nucl. Phys. B **855**, 153 (2012). https://doi.org/10.1016/j.nuclphysb.2011.09.024. arXiv:1107.2652
42. NNPDF Collaboration, Parton distributions for the LHC Run II. JHEP **04**, 040 (2015). https://doi.org/10.1007/JHEP04(2015)040. arXiv:1410.8849

43. NNPDF Collaboration, Parton distributions with QED corrections. Nucl. Phys. B **877**, 290 (2013). https://doi.org/10.1016/j.nuclphysb.2013.10.010. arXiv:1308.0598
44. NNPDF Collaboration, Parton distributions from high-precision collider data. Eur. Phys. J. C **77**, 663 (2017). https://doi.org/10.1140/epjc/s10052-017-5199-5. arXiv:1706.00428
45. T. Sjöstrand et al., An introduction to PYTHIA 8.2. Comput. Phys. Commun. **191**, 159 (2015). https://doi.org/10.1016/j.cpc.2015.01.024. arXiv:1410.3012
46. CMS Collaboration, Event generator tunes obtained from underlying event and multiparton scattering measurements. Eur. Phys. J. C **76**, 155 (2016). https://doi.org/10.1140/epjc/s10052-016-3988-x. arXiv:1512.00815
47. P. Skands, S. Carrazza, J. Rojo, Tuning PYTHIA 8.1: the Monash, tune. Eur. Phys. J. C **74**(2014), 3024 (2013). https://doi.org/10.1140/epjc/s10052-014-3024-y. arXiv:1404.5630
48. CMS Collaboration, Extraction and validation of a new set of CMS pythia8 tunes from underlying-event measurements. Eur. Phys. J. C **80**, 4 (2020). https://doi.org/10.1140/epjc/s10052-019-7499-4. arXiv:1903.12179
49. M. Czakon, A. Mitov, TOP++: a program for the calculation of the top-pair cross-section at hadron colliders. Comput. Phys. Commun. **185**, 2930 (2014). https://doi.org/10.1016/j.cpc.2014.06.021. arXiv:1112.5675
50. R. Gavin, Y. Li, F. Petriello, S. Quackenbush, FEWZ 2.0: a code for hadronic Z production at next-to-next-to-leading order. Comput. Phys. Commun. **182**, 2388 (2011). https://doi.org/10.1016/j.cpc.2011.06.008. arXiv:1011.3540
51. R. Gavin, Y. Li, F. Petriello, S. Quackenbush, W physics at the LHC with FEWZ 2.1. Comput. Phys. Commun. **184**, 208 (2013). https://doi.org/10.1016/j.cpc.2012.09.005. arXiv:1201.5896
52. Y. Li, F. Petriello, Combining QCD and electroweak corrections to dilepton production in FEWZ. Phys. Rev. D **86**, 094034 (2012). https://doi.org/10.1103/PhysRevD.86.094034. arXiv:1208.5967
53. CMS Collaboration, Measurement of the inelastic proton–proton cross section at $\sqrt{s} = 13$ TeV. JHEP **07**, 161 (2018). https://doi.org/10.1007/JHEP07(2018)161. arXiv:1802.02613
54. GEANT4 Collaboration, GEANT4—a simulation toolkit. Nucl. Instrum. Meth. A **506**, 250 (2003). https://doi.org/10.1016/S0168-9002(03)01368-8
55. CMS Collaboration, Particle-flow reconstruction and global event description with the CMS detector. JINST **12**, P10003 (2017). https://doi.org/10.1088/1748-0221/12/10/P10003. arXiv:1706.04965
56. M. Cacciari, G.P. Salam, G. Soyez, The anti-k_T jet clustering algorithm. JHEP **04**, 063 (2008). https://doi.org/10.1088/1126-6708/2008/04/063. arXiv:0802.1189
57. M. Cacciari, G.P. Salam, G. Soyez, FastJet user manual. Eur. Phys. J. C **72**, 1896 (2012). https://doi.org/10.1140/epjc/s10052-012-1896-2. arXiv:1111.6097
58. CMS Collaboration, Technical proposal for the Phase-II upgrade of the Compact Muon Solenoid, CMS Technical Proposal CERN-LHCC-2015-010, CMS-TDR-15-02 (2015). http://cds.cern.ch/record/2020886
59. CMS Collaboration, Pileup mitigation at CMS in 13 TeV data. JINST **15**, P09018 (2020). https://doi.org/10.1088/1748-0221/15/09/p09018. arXiv:2003.00503
60. D. Bertolini, P. Harris, M. Low, N. Tran, Pileup per particle identification. JHEP **10**, 059 (2014). https://doi.org/10.1007/JHEP10(2014)059. arXiv:1407.6013
61. CMS Collaboration, Jet energy scale and resolution in the CMS experiment in pp collisions at 8 TeV. JINST **12**, P02014 (2017). https://doi.org/10.1088/1748-0221/12/02/P02014. arXiv:1607.03663
62. CMS Collaboration, Jet energy scale and resolution performance with 13 TeV data collected by CMS in 2016, Detector Performance Report CMS-DP-2018-028 (2018). http://cds.cern.ch/record/2622157
63. CMS Collaboration, Jet performance in pp collisions at $\sqrt{s} = 7$ TeV, CMS Physics Analysis Summary CMS-PAS-JME-10-003 (2010). http://cdsweb.cern.ch/record/1279362
64. CMS Collaboration, Jet algorithms performance in 13 TeV data, CMS Physics Analysis Summary CMS-PAS-JME-16-003 (2017). http://cds.cern.ch/record/2256875
65. CMS Collaboration, Identification of heavy-flavour jets with the CMS detector in pp collisions at 13 TeV. JINST **13**, P05011 (2018). https://doi.org/10.1088/1748-0221/13/05/P05011. arXiv:1712.07158
66. T. Adams et al., Beam test evaluation of electromagnetic calorimeter modules made from proton-damaged $PbWO_4$ crystals. JINST **11**, P04012 (2016). https://doi.org/10.1088/1748-0221/11/04/P04012
67. A.J. Larkoski, S. Marzani, G. Soyez, J. Thaler, Soft drop. JHEP **05**, 146 (2014). https://doi.org/10.1007/JHEP05(2014)146. arXiv:1402.2657
68. ATLAS and CMS Collaborations, Procedure for the LHC Higgs boson search combination in summer 2011, ATLAS/CMS joint note ATL-PHYS-PUB-2011-011, CMS-NOTE-2011-005 (2011). http://cds.cern.ch/record/1379837
69. T. Junk, Confidence level computation for combining searches with small statistics. Nucl. Instrum. Meth. A **434**, 435 (1999). https://doi.org/10.1016/S0168-9002(99)00498-2. arXiv:hep-ex/9902006
70. A.L. Read, Presentation of search results: the CL_s technique. J. Phys. G **28**, 2693 (2002). https://doi.org/10.1088/0954-3899/28/10/313
71. HEPData record for this analysis (2022). https://doi.org/10.17182/hepdata.114359

CMS Collaboration

Yerevan Physics Institute, Yerevan, Armenia
A. Tumasyan[1]

Institut für Hochenergiephysik, Vienna, Austria
W. Adam, J. W. Andrejkovic, T. Bergauer, S. Chatterjee, K. Damanakis, M. Dragicevic, A. Escalante Del Valle, R. Frühwirth[2], M. Jeitler[2], N. Krammer, L. Lechner, D. Liko, I. Mikulec, P. Paulitsch, F. M. Pitters, J. Schieck[2], R. Schöfbeck, D. Schwarz, S. Templ, W. Waltenberger, C.-E. Wulz[2]

Universiteit Antwerpen, Antwerpen, Belgium
M. R. Darwish[3], E. A. De Wolf, T. Janssen, T. Kello[4], A. Lelek, H. Rejeb Sfar, P. Van Mechelen, S. Van Putte, N. Van Remortel

Vrije Universiteit Brussel, Brussels, Belgium
E. S. Bols, J. D'Hondt, A. De Moor, M. Delcourt, H. El Faham, S. Lowette, S. Moortgat, A. Morton, D. Müller, A. R. Sahasransu, S. Tavernier, W. Van Doninck, D. Vannerom

Université Libre de Bruxelles, Brussels, Belgium
D. Beghin, B. Bilin, B. Clerbaux, G. De Lentdecker, L. Favart, A. K. Kalsi, K. Lee, M. Mahdavikhorrami, I. Makarenko, L. Moureaux, S. Paredes, L. Pétré, A. Popov, N. Postiau, E. Starling, L. Thomas, M. Vanden Bemden, C. Vander Velde, P. Vanlaer

Ghent University, Ghent, Belgium
T. Cornelis, D. Dobur, J. Knolle, L. Lambrecht, G. Mestdach, M. Niedziela, C. Rendón, C. Roskas, A. Samalan, K. Skovpen, M. Tytgat, B. Vermassen, L. Wezenbeek

Université Catholique de Louvain, Louvain-la-Neuve, Belgium
A. Benecke, A. Bethani, G. Bruno, F. Bury, C. Caputo, P. David, C. Delaere, I. S. Donertas, A. Giammanco, K. Jaffel, Sa. Jain, V. Lemaitre, K. Mondal, J. Prisciandaro, A. Taliercio, M. Teklishyn, T. T. Tran, P. Vischia, S. Wertz

Centro Brasileiro de Pesquisas Fisicas, Rio de Janeiro, Brazil
G. A. Alves, C. Hensel, A. Moraes, P. Rebello Teles

Universidade do Estado do Rio de Janeiro, Rio de Janeiro, Brazil
W. L. Aldá Júnior, M. Alves Gallo Pereira, M. Barroso Ferreira Filho, H. Brandao Malbouisson, W. Carvalho, J. Chinellato[5], E. M. Da Costa, G. G. Da Silveira[6], D. De Jesus Damiao, V. Dos Santos Sousa, S. Fonseca De Souza, C. Mora Herrera, K. Mota Amarilo, L. Mundim, H. Nogima, A. Santoro, S. M. Silva Do Amaral, A. Sznajder, M. Thiel, F. Torres Da Silva De Araujo[7], A. Vilela Pereira

Universidade Estadual Paulista, Universidade Federal do ABC, São Paulo, Brazil
C. A. Bernardes[6], L. Calligaris, T. R. Fernandez Perez Tomei, E. M. Gregores, D. S. Lemos, P. G. Mercadante, S. F. Novaes, Sandra S. Padula

Institute for Nuclear Research and Nuclear Energy, Bulgarian Academy of Sciences, Sofia, Bulgaria
A. Aleksandrov, G. Antchev, R. Hadjiiska, P. Iaydjiev, M. Misheva, M. Rodozov, M. Shopova, G. Sultanov

University of Sofia, Sofia, Bulgaria
A. Dimitrov, T. Ivanov, L. Litov, B. Pavlov, P. Petkov, A. Petrov

Beihang University, Beijing, China
T. Cheng, T. Javaid[8], M. Mittal, L. Yuan

Department of Physics, Tsinghua University, Beijing, China
M. Ahmad, G. Bauer, C. Dozen, Z. Hu, J. Martins[9], Y. Wang, K. Yi[10,11]

Institute of High Energy Physics, Beijing, China
E. Chapon, G. M. Chen[8], H. S. Chen[8], M. Chen, F. Iemmi, A. Kapoor, D. Leggat, H. Liao, Z.-A. Liu[12], V. Milosevic, F. Monti, R. Sharma, J. Tao, J. Thomas-Wilsker, J. Wang, H. Zhang, J. Zhao

State Key Laboratory of Nuclear Physics and Technology, Peking University, Beijing, China
A. Agapitos, Y. An, Y. Ban, C. Chen, A. Levin, Q. Li, X. Lyu, Y. Mao, S. J. Qian, D. Wang, J. Xiao, H. Yang

Sun Yat-Sen University, Guangzhou, China
M. Lu, Z. You

Institute of Modern Physics and Key Laboratory of Nuclear Physics and Ion-beam Application (MOE), Fudan University, Shanghai, China
X. Gao[4], H. Okawa, Y. Zhang

Zhejiang University, Hangzhou, Zhejiang, China
Z. Lin, M. Xiao

Universidad de Los Andes, Bogota, Colombia
C. Avila, A. Cabrera, C. Florez, J. Fraga

Universidad de Antioquia, Medellin, Colombia
J. Mejia Guisao, F. Ramirez, J. D. Ruiz Alvarez

Faculty of Electrical Engineering, Mechanical Engineering and Naval Architecture, University of Split, Split, Croatia
D. Giljanovic, N. Godinovic, D. Lelas, I. Puljak

Faculty of Science, University of Split, Split, Croatia
Z. Antunovic, M. Kovac, T. Sculac

Institute Rudjer Boskovic, Zagreb, Croatia
V. Brigljevic, D. Ferencek, D. Majumder, M. Roguljic, A. Starodumov[13], T. Susa

University of Cyprus, Nicosia, Cyprus
A. Attikis, K. Christoforou, A. Ioannou, G. Kole, M. Kolosova, S. Konstantinou, J. Mousa, C. Nicolaou, F. Ptochos, P. A. Razis, H. Rykaczewski, H. Saka

Charles University, Prague, Czech Republic
M. Finger[13], M. Finger Jr.[13], A. Kveton

Escuela Politecnica Nacional, Quito, Ecuador
E. Ayala

Universidad San Francisco de Quito, Quito, Ecuador
E. Carrera Jarrin

Academy of Scientific Research and Technology of the Arab Republic of Egypt, Egyptian Network of High Energy Physics, Cairo, Egypt
A. A. Abdelalim[14,15], S. Elgammal[16]

Center for High Energy Physics (CHEP-FU), Fayoum University, El-Fayoum, Egypt
M. A. Mahmoud, Y. Mohammed

National Institute of Chemical Physics and Biophysics, Tallinn, Estonia
S. Bhowmik, R. K. Dewanjee, K. Ehataht, M. Kadastik, S. Nandan, C. Nielsen, J. Pata, M. Raidal, L. Tani, C. Veelken

Department of Physics, University of Helsinki, Helsinki, Finland
P. Eerola, H. Kirschenmann, K. Osterberg, M. Voutilainen

Helsinki Institute of Physics, Helsinki, Finland
S. Bharthuar, E. Brücken, F. Garcia, J. Havukainen, M. S. Kim, R. Kinnunen, T. Lampén,

K. Lassila-Perini, S. Lehti, T. Lindén, M. Lotti, L. Martikainen, M. Myllymäki, J. Ott, H. Siikonen, E. Tuominen, J. Tuominiemi

Lappeenranta-Lahti University of Technology, Lappeenranta, Finland
P. Luukka, H. Petrow, T. Tuuva

IRFU, CEA, Université Paris-Saclay, Gif-sur-Yvette, France
C. Amendola, M. Besancon, F. Couderc, M. Dejardin, D. Denegri, J. L. Faure, F. Ferri, S. Ganjour, P. Gras, G. Hamel de Monchenault, P. Jarry, B. Lenzi, E. Locci, J. Malcles, J. Rander, A. Rosowsky, M.Ö. Sahin, A. Savoy-Navarro[17], M. Titov, G. B. Yu

Laboratoire Leprince-Ringuet, CNRS/IN2P3, Ecole Polytechnique, Institut Polytechnique de Paris, Palaiseau, France
S. Ahuja, F. Beaudette, M. Bonanomi, A. Buchot Perraguin, P. Busson, A. Cappati, C. Charlot, O. Davignon, B. Diab, G. Falmagne, S. Ghosh, R. Granier de Cassagnac, A. Hakimi, I. Kucher, J. Motta, M. Nguyen, C. Ochando, P. Paganini, J. Rembser, R. Salerno, U. Sarkar, J. B. Sauvan, Y. Sirois, A. Tarabini, A. Zabi, A. Zghiche

Université de Strasbourg, CNRS, IPHC UMR 7178, Strasbourg, France
J.-L. Agram[18], J. Andrea, D. Apparu, D. Bloch, G. Bourgatte, J.-M. Brom, E. C. Chabert, C. Collard, D. Darej, J.-C. Fontaine[18], U. Goerlach, C. Grimault, A.-C. Le Bihan, E. Nibigira, P. Van Hove

Institut de Physique des 2 Infinis de Lyon (IP2I), Villeurbanne, France
E. Asilar, S. Beauceron, C. Bernet, G. Boudoul, C. Camen, A. Carle, N. Chanon, D. Contardo, P. Depasse, H. El Mamouni, J. Fay, S. Gascon, M. Gouzevitch, B. Ille, I. B. Laktineh, H. Lattaud, A. Lesauvage, M. Lethuillier, L. Mirabito, S. Perries, K. Shchablo, V. Sordini, L. Torterotot, G. Touquet, M. Vander Donckt, S. Viret

Georgian Technical University, Tbilisi, Georgia
I. Bagaturia[19], I. Lomidze, Z. Tsamalaidze[13]

RWTH Aachen University, I. Physikalisches Institut, Aachen, Germany
V. Botta, L. Feld, K. Klein, M. Lipinski, D. Meuser, A. Pauls, N. Röwert, J. Schulz, M. Teroerde

RWTH Aachen University, III. Physikalisches Institut A, Aachen, Germany
A. Dodonova, D. Eliseev, M. Erdmann, P. Fackeldey, B. Fischer, T. Hebbeker, K. Hoepfner, F. Ivone, L. Mastrolorenzo, M. Merschmeyer, A. Meyer, G. Mocellin, S. Mondal, S. Mukherjee, D. Noll, A. Novak, A. Pozdnyakov, Y. Rath, H. Reithler, A. Schmidt, S. C. Schuler, A. Sharma, L. Vigilante, S. Wiedenbeck, S. Zaleski

RWTH Aachen University, III. Physikalisches Institut B, Aachen, Germany
C. Dziwok, G. Flügge, W. Haj Ahmad[20], O. Hlushchenko, T. Kress, A. Nowack, O. Pooth, D. Roy, A. Stahl, T. Ziemons, A. Zotz

Deutsches Elektronen-Synchrotron, Hamburg, Germany
H. Aarup Petersen, M. Aldaya Martin, P. Asmuss, S. Baxter, M. Bayatmakou, O. Behnke, A. Bermúdez Martínez, S. Bhattacharya, A. A. Bin Anuar, F. Blekman, K. Borras[21], D. Brunner, A. Campbell, A. Cardini, C. Cheng, F. Colombina, S. Consuegra Rodríguez, G. Correia Silva, V. Danilov, M. De Silva, L. Didukh, G. Eckerlin, D. Eckstein, L. I. Estevez Banos, O. Filatov, E. Gallo[22], A. Geiser, A. Giraldi, A. Grohsjean, M. Guthoff, A. Jafari[23], N. Z. Jomhari, A. Kasem[21], M. Kasemann, H. Kaveh, C. Kleinwort, R. Kogler, D. Krücker, W. Lange, K. Lipka, W. Lohmann[24], R. Mankel, I.-A. Melzer-Pellmann, M. Mendizabal Morentin, J. Metwally, A. B. Meyer, M. Meyer, J. Mnich, A. Mussgiller, A. Nürnberg, Y. Otarid, D. Pérez Adán, D. Pitzl, A. Raspereza, B. Ribeiro Lopes, J. Rübenach, A. Saggio, A. Saibel, M. Savitskyi, M. Scham[25], V. Scheurer, S. Schnake, P. Schütze, C. Schwanenberger[22], M. Shchedrolosiev, R. E. Sosa Ricardo, D. Stafford, N. Tonon, M. Van De Klundert, F. Vazzoler, R. Walsh, D. Walter, Q. Wang, Y. Wen, K. Wichmann, L. Wiens, C. Wissing, S. Wuchterl

University of Hamburg, Hamburg, Germany
R. Aggleton, S. Albrecht, S. Bein, L. Benato, P. Connor, K. De Leo, M. Eich, K. El Morabit, F. Feindt,

A. Fröhlich, C. Garbers, E. Garutti, P. Gunnellini, M. Hajheidari, J. Haller, A. Hinzmann, G. Kasieczka, R. Klanner, T. Kramer, V. Kutzner, J. Lange, T. Lange, A. Lobanov, A. Malara, A. Mehta, A. Nigamova, K. J. Pena Rodriguez, M. Rieger, O. Rieger, P. Schleper, M. Schröder, J. Schwandt, J. Sonneveld, H. Stadie, G. Steinbrück, A. Tews, I. Zoi

Karlsruher Institut fuer Technologie, Karlsruhe, Germany
J. Bechtel, S. Brommer, M. Burkart, E. Butz, R. Caspart, T. Chwalek, W. De Boer[†], A. Dierlamm, A. Droll, N. Faltermann, M. Giffels, J. O. Gosewisch, A. Gottmann, F. Hartmann[26], C. Heidecker, U. Husemann, P. Keicher, R. Koppenhöfer, S. Maier, M. Metzler, S. Mitra, Th. Müller, M. Neukum, G. Quast, K. Rabbertz, J. Rauser, D. Savoiu, M. Schnepf, D. Seith, I. Shvetsov, H. J. Simonis, R. Ulrich, J. Van Der Linden, R. F. Von Cube, M. Wassmer, M. Weber, S. Wieland, R. Wolf, S. Wozniewski, S. Wunsch

Institute of Nuclear and Particle Physics (INPP), NCSR Demokritos, Aghia Paraskevi, Greece
G. Anagnostou, G. Daskalakis, A. Kyriakis, A. Stakia

National and Kapodistrian University of Athens, Athens, Greece
M. Diamantopoulou, D. Karasavvas, P. Kontaxakis, C. K. Koraka, A. Manousakis-Katsikakis, A. Panagiotou, I. Papavergou, N. Saoulidou, K. Theofilatos, E. Tziaferi, K. Vellidis, E. Vourliotis

National Technical University of Athens, Athens, Greece
G. Bakas, K. Kousouris, I. Papakrivopoulos, G. Tsipolitis, A. Zacharopoulou

University of Ioánnina, Ioánnina, Greece
K. Adamidis, I. Bestintzanos, I. Evangelou, C. Foudas, P. Gianneios, P. Katsoulis, P. Kokkas, N. Manthos, I. Papadopoulos, J. Strologas

MTA-ELTE Lendület CMS Particle and Nuclear Physics Group, Eötvös Loránd University, Budapest, Hungary
M. Csanád, K. Farkas, M. M. A. Gadallah[27], S. Lökös[28], P. Major, K. Mandal, G. Pásztor, A. J. Rádl, O. Surányi, G. I. Veres

Wigner Research Centre for Physics, Budapest, Hungary
M. Bartók[29], G. Bencze, C. Hajdu, D. Horvath[30,31], F. Sikler, V. Veszpremi

Institute of Nuclear Research ATOMKI, Debrecen, Hungary
S. Czellar, D. Fasanella, F. Fienga, J. Karancsi[29], J. Molnar, Z. Szillasi, D. Teyssier

Institute of Physics, University of Debrecen, Debrecen, Hungary
P. Raics, Z. L. Trocsanyi[32], B. Ujvari

Karoly Robert Campus, MATE Institute of Technology, Gyongyos, Hungary
T. Csorgo[33], F. Nemes[33], T. Novak

Panjab University, Chandigarh, India
S. Bansal, S. B. Beri, V. Bhatnagar, G. Chaudhary, S. Chauhan, N. Dhingra[34], R. Gupta, A. Kaur, H. Kaur, M. Kaur, P. Kumari, M. Meena, K. Sandeep, J. B. Singh[35], A. K. Virdi

University of Delhi, Delhi, India
A. Ahmed, A. Bhardwaj, B. C. Choudhary, M. Gola, S. Keshri, A. Kumar, M. Naimuddin, P. Priyanka, K. Ranjan, A. Shah

Saha Institute of Nuclear Physics, HBNI, Kolkata, India
M. Bharti[36], R. Bhattacharya, S. Bhattacharya, D. Bhowmik, S. Dutta, S. Dutta, B. Gomber[37], M. Maity[38], P. Palit, P. K. Rout, G. Saha, B. Sahu, S. Sarkar, M. Sharan

Indian Institute of Technology Madras, Madras, India
P. K. Behera, S. C. Behera, P. Kalbhor, J. R. Komaragiri[39], D. Kumar[39], A. Muhammad, L. Panwar[39], R. Pradhan, P. R. Pujahari, A. Sharma, A. K. Sikdar, P. C. Tiwari[39]

Bhabha Atomic Research Centre, Mumbai, India
K. Naskar[40]

Tata Institute of Fundamental Research-A, Mumbai, India
T. Aziz, S. Dugad, M. Kumar, G. B. Mohanty

Tata Institute of Fundamental Research-B, Mumbai, India
S. Banerjee, R. Chudasama, M. Guchait, S. Karmakar, S. Kumar, G. Majumder, K. Mazumdar, S. Mukherjee

National Institute of Science Education and Research, An OCC of Homi Bhabha National Institute, Bhubaneswar, Odisha, India
S. Bahinipati[41], C. Kar, P. Mal, T. Mishra, V. K. Muraleedharan Nair Bindhu[42], A. Nayak[42], P. Saha, N. Sur, S. K. Swain, D. Vats[42]

Indian Institute of Science Education and Research (IISER), Pune, India
A. Alpana, S. Dube, B. Kansal, A. Laha, S. Pandey, A. Rastogi, S. Sharma

Isfahan University of Technology, Isfahan, Iran
H. Bakhshiansohi[43], E. Khazaie, M. Zeinali[44]

Institute for Research in Fundamental Sciences (IPM), Tehran, Iran
S. Chenarani[45], S. M. Etesami, M. Khakzad, M. Mohammadi Najafabadi

University College Dublin, Dublin, Ireland
M. Grunewald

INFN Sezione di Bari[a], Università di Bari[b], Politecnico di Bari[c], Bari, Italy
M. Abbrescia[a,b], R. Aly[a,c,14], C. Aruta[a,b], A. Colaleo[a], D. Creanza[a,c], N. De Filippis[a,c], M. De Palma[a,b], A. Di Florio[a,b], A. Di Pilato[a,b], W. Elmetenawee[a,b], F. Errico[a,b], L. Fiore[a], A. Gelmi[a,b], G. Iaselli[a,c], M. Ince[a,b], S. Lezki[a,b], G. Maggi[a,c], M. Maggi[a], I. Margjeka[a,b], V. Mastrapasqua[a,b], S. My[a,b], S. Nuzzo[a,b], A. Pellecchia[a,b], A. Pompili[a,b], G. Pugliese[a,c], D. Ramos[a], A. Ranieri[a], G. Selvaggi[a,b], L. Silvestris[a], F. M. Simone[a,b], Ü. Sözbilir[a], R. Venditti[a], P. Verwilligen[a]

INFN Sezione di Bologna[a], Università di Bologna[b], Bologna, Italy
G. Abbiendi[a], C. Battilana[a,b], D. Bonacorsi[a,b], L. Borgonovi[a], L. Brigliadori[a], R. Campanini[a,b], P. Capiluppi[a,b], A. Castro[a,b], F. R. Cavallo[a], C. Ciocca[a], M. Cuffiani[a,b], G. M. Dallavalle[a], T. Diotalevi[a,b], F. Fabbri[a], A. Fanfani[a,b], P. Giacomelli[a], L. Giommi[a,b], C. Grandi[a], L. Guiducci[a,b], S. Lo Meo[a,46], L. Lunerti[a,b], S. Marcellini[a], G. Masetti[a], F. L. Navarria[a,b], A. Perrotta[a], F. Primavera[a,b], A. M. Rossi[a,b], T. Rovelli[a,b], G. P. Siroli[a,b]

INFN Sezione di Catania[a], Università di Catania[b], Catania, Italy
S. Albergo[a,b,47], S. Costa[a,b,47], A. Di Mattia[a], R. Potenza[a,b], A. Tricomi[a,b,47], C. Tuve[a,b]

INFN Sezione di Firenze[a], Università di Firenze[b], Florence, Italy
G. Barbagli[a], A. Cassese[a], R. Ceccarelli[a,b], V. Ciulli[a,b], C. Civinini[a], R. D'Alessandro[a,b], E. Focardi[a,b], G. Latino[a,b], P. Lenzi[a,b], M. Lizzo[a,b], M. Meschini[a], S. Paoletti[a], R. Seidita[a,b], G. Sguazzoni[a], L. Viliani[a]

INFN Laboratori Nazionali di Frascati, Frascati, Italy
L. Benussi, S. Bianco, D. Piccolo

INFN Sezione di Genova[a], Università di Genova[b], Genoa, Italy
M. Bozzo[a,b], F. Ferro[a], R. Mulargia[a], E. Robutti[a], S. Tosi[a,b]

INFN Sezione di Milano-Bicocca[a], Università di Milano-Bicocca[b], Milan, Italy
A. Benaglia[a], G. Boldrini[a], F. Brivio[a,b], F. Cetorelli[a,b], F. De Guio[a,b], M. E. Dinardo[a,b], P. Dini[a], S. Gennai[a], A. Ghezzi[a,b], P. Govoni[a,b], L. Guzzi[a,b], M. T. Lucchini[a,b], M. Malberti[a], S. Malvezzi[a], A. Massironi[a], D. Menasce[a], L. Moroni[a], M. Paganoni[a,b], D. Pedrini[a], B. S. Pinolini[a], S. Ragazzi[a,b], N. Redaelli[a], T. Tabarelli de Fatis[a,b], D. Valsecchi[a,b,26], D. Zuolo[a,b]

INFN Sezione di Napoli[a], Università di Napoli 'Federico II'[b], Naples, Italy; Università della Basilicata[c], Potenza, Italy; Università G. Marconi[d], Rome, Italy

S. Buontempo[a], F. Carnevali[a,b], N. Cavallo[a,c], A. De Iorio[a,b], F. Fabozzi[a,c], A. O. M. Iorio[a,b], L. Lista[a,b,48], S. Meola[a,d,26], P. Paolucci[a,26], B. Rossi[a], C. Sciacca[a,b]

INFN Sezione di Padova[a], Università di Padova[b], Padua, Italy; Università di Trento[c], Trento, Italy
P. Azzi[a], N. Bacchetta[a], D. Bisello[a,b], P. Bortignon[a], A. Bragagnolo[a,b], R. Carlin[a,b], P. Checchia[a], T. Dorigo[a], U. Dosselli[a], F. Gasparini[a,b], U. Gasparini[a,b], G. Grosso[a], L. Layer[a,49], E. Lusiani[a], M. Margoni[a,b], A. T. Meneguzzo[a,b], J. Pazzini[a,b], P. Ronchese[a,b], R. Rossin[a,b], F. Simonetto[a,b], G. Strong[a], M. Tosi[a,b], H. Yarar[a,b], M. Zanetti[a,b], P. Zotto[a,b], A. Zucchetta[a,b], G. Zumerle[a,b]

INFN Sezione di Pavia[a], Università di Pavia[b], Pavia, Italy
C. Aimè[a,b], A. Braghieri[a], S. Calzaferri[a,b], D. Fiorina[a,b], P. Montagna[a,b], S. P. Ratti[a,b], V. Re[a], C. Riccardi[a,b], P. Salvini[a], I. Vai[a], P. Vitulo[a,b]

INFN Sezione di Perugia[a], Università di Perugia[b], Perugia, Italy
P. Asenov[a,50], G. M. Bilei[a], D. Ciangottini[a,b], L. Fanò[a,b], M. Magherini[a,b], G. Mantovani[a,b], V. Mariani[a,b], M. Menichelli[a], F. Moscatelli[a,50], A. Piccinelli[a,b], M. Presilla[a,b], A. Rossi[a,b], A. Santocchia[a,b], D. Spiga[a], T. Tedeschi[a,b]

INFN Sezione di Pisa[a], Università di Pisa[b], Scuola Normale Superiore di Pisa[c], Pisa, Italy; Università di Siena[d], Siena, Italy
P. Azzurri[a], G. Bagliesi[a], V. Bertacchi[a,c], L. Bianchini[a], T. Boccali[a], E. Bossini[a,b], R. Castaldi[a], M. A. Ciocci[a,b], V. D'Amante[a,d], R. Dell'Orso[a], M. R. Di Domenico[a,d], S. Donato[a], A. Giassi[a], F. Ligabue[a,c], E. Manca[a,c], G. Mandorli[a,c], D. Matos Figueiredo[a], A. Messineo[a,b], M. Musich[a], F. Palla[a], S. Parolia[a,b], G. Ramirez-Sanchez[a,c], A. Rizzi[a,b], G. Rolandi[a,c], S. Roy Chowdhury[a,c], A. Scribano[a], N. Shafiei[a,b], P. Spagnolo[a], R. Tenchini[a], G. Tonelli[a,b], N. Turini[a,d], A. Venturi[a], P. G. Verdini[a]

INFN Sezione di Roma[a], Sapienza Università di Roma[b], Rome, Italy
P. Barria[a], M. Campana[a,b], F. Cavallari[a], D. Del Re[a,b], E. Di Marco[a], M. Diemoz[a], E. Longo[a,b], P. Meridiani[a], G. Organtini[a,b], F. Pandolfi[a], R. Paramatti[a,b], C. Quaranta[a,b], S. Rahatlou[a,b], C. Rovelli[a], F. Santanastasio[a,b], L. Soffi[a], R. Tramontano[a,b]

INFN Sezione di Torino[a], Università di Torino[b], Turin, Italy; Università del Piemonte Orientale[c], Novara, Italy
N. Amapane[a,b], R. Arcidiacono[a,c], S. Argiro[a,b], M. Arneodo[a,c], N. Bartosik[a], R. Bellan[a,b], A. Bellora[a,b], J. Berenguer Antequera[a,b], C. Biino[a], N. Cartiglia[a], M. Costa[a,b], R. Covarelli[a,b], N. Demaria[a], B. Kiani[a,b], F. Legger[a], C. Mariotti[a], S. Maselli[a], E. Migliore[a,b], E. Monteil[a,b], M. Monteno[a], M. M. Obertino[a,b], G. Ortona[a], L. Pacher[a,b], N. Pastrone[a], M. Pelliccioni[a], M. Ruspa[a,c], K. Shchelina[a], F. Siviero[a,b], V. Sola[a], A. Solano[a,b], D. Soldi[a,b], A. Staiano[a], M. Tornago[a,b], D. Trocino[a], A. Vagnerini[a,b]

INFN Sezione di Trieste[a], Università di Trieste[b], Trieste, Italy
S. Belforte[a], V. Candelise[a,b], M. Casarsa[a], F. Cossutti[a], A. Da Rold[a,b], G. Della Ricca[a,b], G. Sorrentino[a,b]

Kyungpook National University, Daegu, Korea
S. Dogra, C. Huh, B. Kim, D. H. Kim, G. N. Kim, J. Kim, J. Lee, S. W. Lee, C. S. Moon, Y. D. Oh, S. I. Pak, S. Sekmen, Y. C. Yang

Chonnam National University, Institute for Universe and Elementary Particles, Kwangju, Korea
H. Kim, D. H. Moon

Hanyang University, Seoul, Korea
B. Francois, T. J. Kim, J. Park

Korea University, Seoul, Korea
S. Cho, S. Choi, B. Hong, K. Lee, K. S. Lee, J. Lim, J. Park, S. K. Park, J. Yoo

Department of Physics, Kyung Hee University, Seoul, Korea
J. Goh, A. Gurtu

Sejong University, Seoul, Korea
H. S. Kim, Y. Kim

Seoul National University, Seoul, Korea
J. Almond, J. H. Bhyun, J. Choi, S. Jeon, J. Kim, J. S. Kim, S. Ko, H. Kwon, H. Lee, S. Lee, B. H. Oh, M. Oh, S. B. Oh, H. Seo, U. K. Yang, I. Yoon

University of Seoul, Seoul, Korea
W. Jang, D. Y. Kang, Y. Kang, S. Kim, B. Ko, J. S. H. Lee, Y. Lee, J. A. Merlin, I. C. Park, Y. Roh, M. S. Ryu, D. Song, I. J. Watson, S. Yang

Department of Physics, Yonsei University, Seoul, Korea
S. Ha, H. D. Yoo

Sungkyunkwan University, Suwon, Korea
M. Choi, H. Lee, Y. Lee, I. Yu

College of Engineering and Technology, American University of the Middle East (AUM), Dasman, Kuwait
T. Beyrouthy, Y. Maghrbi

Riga Technical University, Riga, Latvia
K. Dreimanis, V. Veckalns

Vilnius University, Vilnius, Lithuania
M. Ambrozas, A. Carvalho Antunes De Oliveira, A. Juodagalvis, A. Rinkevicius, G. Tamulaitis

National Centre for Particle Physics, Universiti Malaya, Kuala Lumpur, Malaysia
N. Bin Norjoharuddeen, Z. Zolkapli

Universidad de Sonora (UNISON), Hermosillo, Mexico
J. F. Benitez, A. Castaneda Hernandez, H. A. Encinas Acosta, L. G. Gallegos Maríñez, M. León Coello, J. A. Murillo Quijada, A. Sehrawat, L. Valencia Palomo

Centro de Investigacion y de Estudios Avanzados del IPN, Mexico City, Mexico
G. Ayala, H. Castilla-Valdez, E. De La Cruz-Burelo, I. Heredia-De La Cruz[51], R. Lopez-Fernandez, C. A. Mondragon Herrera, D. A. Perez Navarro, R. Reyes-Almanza, A. Sánchez Hernández

Universidad Iberoamericana, Mexico City, Mexico
S. Carrillo Moreno, C. Oropeza Barrera, F. Vazquez Valencia

Benemerita Universidad Autonoma de Puebla, Puebla, Mexico
I. Pedraza, H. A. Salazar Ibarguen, C. Uribe Estrada

University of Montenegro, Podgorica, Montenegro
J. Mijuskovic[52], N. Raicevic

University of Auckland, Auckland, New Zealand
D. Krofcheck

University of Canterbury, Christchurch, New Zealand
P. H. Butler

National Centre for Physics, Quaid-I-Azam University, Islamabad, Pakistan
A. Ahmad, M. I. Asghar, A. Awais, M. I. M. Awan, M. Gul, H. R. Hoorani, W. A. Khan, M. A. Shah, M. Shoaib, M. Waqas

Faculty of Computer Science, Electronics and Telecommunications, AGH University of Science and Technology, Krakow, Poland
V. Avati, L. Grzanka, M. Malawski

National Centre for Nuclear Research, Swierk, Poland
H. Bialkowska, M. Bluj, B. Boimska, M. Górski, M. Kazana, M. Szleper, P. Zalewski

Institute of Experimental Physics, Faculty of Physics, University of Warsaw, Warsaw, Poland
K. Bunkowski, K. Doroba, A. Kalinowski, M. Konecki, J. Krolikowski

Laboratório de Instrumentação e Física Experimental de Partículas, Lisbon, Portugal
M. Araujo, P. Bargassa, D. Bastos, A. Boletti, P. Faccioli, M. Gallinaro, J. Hollar, N. Leonardo, T. Niknejad, M. Pisano, J. Seixas, O. Toldaiev, J. Varela

VINCA Institute of Nuclear Sciences, University of Belgrade, Belgrade, Serbia
P. Adzic[53], M. Dordevic, P. Milenovic, J. Milosevic

Centro de Investigaciones Energéticas Medioambientales y Tecnológicas (CIEMAT), Madrid, Spain
M. Aguilar-Benitez, J. Alcaraz Maestre, A. Álvarez Fernández, I. Bachiller, M. Barrio Luna, Cristina F. Bedoya, C. A. Carrillo Montoya, M. Cepeda, M. Cerrada, N. Colino, B. De La Cruz, A. Delgado Peris, J. P. Fernández Ramos, J. Flix, M. C. Fouz, O. Gonzalez Lopez, S. Goy Lopez, J. M. Hernandez, M. I. Josa, J. León Holgado, D. Moran, Á. Navarro Tobar, C. Perez Dengra, A. Pérez-Calero Yzquierdo, J. Puerta Pelayo, I. Redondo, L. Romero, S. Sánchez Navas, L. Urda Gómez, C. Willmott

Universidad Autónoma de Madrid, Madrid, Spain
J. F. de Trocóniz

Instituto Universitario de Ciencias y Tecnologías Espaciales de Asturias (ICTEA), Universidad de Oviedo, Oviedo, Spain
B. Alvarez Gonzalez, J. Cuevas, C. Erice, J. Fernandez Menendez, S. Folgueras, I. Gonzalez Caballero, J. R. González Fernández, E. Palencia Cortezon, C. Ramón Álvarez, V. Rodríguez Bouza, A. Soto Rodríguez, A. Trapote, N. Trevisani, C. Vico Villalba

Instituto de Física de Cantabria (IFCA), CSIC-Universidad de Cantabria, Santander, Spain
J. A. Brochero Cifuentes, I. J. Cabrillo, A. Calderon, J. Duarte Campderros, M. Fernandez, C. Fernandez Madrazo, P. J. Fernández Manteca, A. García Alonso, G. Gomez, C. Martinez Rivero, P. Martinez Ruiz del Arbol, F. Matorras, P. Matorras Cuevas, J. Piedra Gomez, C. Prieels, A. Ruiz-Jimeno, L. Scodellaro, I. Vila, J. M. Vizan Garcia

University of Colombo, Colombo, Sri Lanka
M. K. Jayananda, B. Kailasapathy[54], D. U. J. Sonnadara, D. D. C. Wickramarathna

Department of Physics, University of Ruhuna, Matara, Sri Lanka
W. G. D. Dharmaratna, K. Liyanage, N. Perera, N. Wickramage

CERN, European Organization for Nuclear Research, Geneva, Switzerland
T. K. Aarrestad, D. Abbaneo, J. Alimena, E. Auffray, G. Auzinger, J. Baechler, P. Baillon†, D. Barney, J. Bendavid, M. Bianco, A. Bocci, C. Caillol, T. Camporesi, M. Capeans Garrido, G. Cerminara, N. Chernyavskaya, S. S. Chhibra, S. Choudhury, M. Cipriani, L. Cristella, D. d'Enterria, A. Dabrowski, A. David, A. De Roeck, M. M. Defranchis, M. Deile, M. Dobson, M. Dünser, N. Dupont, A. Elliott-Peisert, F. Fallavollita[55], A. Florent, L. Forthomme, G. Franzoni, W. Funk, S. Ghosh, S. Giani, D. Gigi, K. Gill, F. Glege, L. Gouskos, E. Govorkova, M. Haranko, J. Hegeman, V. Innocente, T. James, P. Janot, J. Kaspar, J. Kieseler, M. Komm, N. Kratochwil, C. Lange, S. Laurila, P. Lecoq, A. Lintuluoto, K. Long, C. Lourenço, B. Maier, L. Malgeri, S. Mallios, M. Mannelli, A. C. Marini, F. Meijers, S. Mersi, E. Meschi, F. Moortgat, M. Mulders, S. Orfanelli, L. Orsini, F. Pantaleo, E. Perez, M. Peruzzi, A. Petrilli, G. Petrucciani, A. Pfeiffer, M. Pierini, D. Piparo, M. Pitt, H. Qu, T. Quast, D. Rabady, A. Racz, G. Reales Gutiérrez, M. Rovere, H. Sakulin, J. Salfeld-Nebgen, S. Scarfi, C. Schäfer, M. Selvaggi, A. Sharma, P. Silva, W. Snoeys, P. Sphicas[56], S. Summers, K. Tatar, V. R. Tavolaro, D. Treille, P. Tropea, A. Tsirou, J. Wanczyk[57], K. A. Wozniak, W. D. Zeuner

Paul Scherrer Institut, Villigen, Switzerland
L. Caminada[58], A. Ebrahimi, W. Erdmann, R. Horisberger, Q. Ingram, H. C. Kaestli, D. Kotlinski, M. Missiroli[58], L. Noehte[58], T. Rohe

ETH Zurich-Institute for Particle Physics and Astrophysics (IPA), Zurich, Switzerland
K. Androsov[57], M. Backhaus, P. Berger, A. Calandri, A. De Cosa, G. Dissertori, M. Dittmar, M. Donegà,

C. Dorfer, F. Eble, K. Gedia, F. Glessgen, T. A. Gómez Espinosa, C. Grab, D. Hits, W. Lustermann, A.-M. Lyon, R. A. Manzoni, L. Marchese, C. Martin Perez, M. T. Meinhard, F. Nessi-Tedaldi, J. Niedziela, F. Pauss, V. Perovic, S. Pigazzini, M. G. Ratti, M. Reichmann, C. Reissel, T. Reitenspiess, B. Ristic, D. Ruini, D. A. Sanz Becerra, V. Stampf, J. Steggemann[57], R. Wallny

Universität Zürich, Zurich, Switzerland
C. Amsler[59], P. Bärtschi, C. Botta, D. Brzhechko, M. F. Canelli, K. Cormier, A. De Wit, R. Del Burgo, J. K. Heikkilä, M. Huwiler, W. Jin, A. Jofrehei, B. Kilminster, S. Leontsinis, S. P. Liechti, A. Macchiolo, P. Meiring, V. M. Mikuni, U. Molinatti, I. Neutelings, A. Reimers, P. Robmann, S. Sanchez Cruz, K. Schweiger, M. Senger, Y. Takahashi

National Central University, Chung-Li, Taiwan
C. Adloff[60], C. M. Kuo, W. Lin, A. Roy, T. Sarkar[38], S. S. Yu

National Taiwan University (NTU), Taipei, Taiwan
L. Ceard, Y. Chao, K. F. Chen, P. H. Chen, P.s. Chen, H. Cheng, W.-S. Hou, Y.y. Li, R.-S. Lu, E. Paganis, A. Psallidas, A. Steen, H.y. Wu, E. Yazgan, P.r. Yu

Department of Physics, Faculty of Science, Chulalongkorn University, Bangkok, Thailand
B. Asavapibhop, C. Asawatangtrakuldee, N. Srimanobhas

Physics Department, Science and Art Faculty, Çukurova University, Adana, Turkey
F. Boran, S. Damarseckin[61], Z. S. Demiroglu, F. Dolek, I. Dumanoglu[62], E. Eskut, Y. Guler[63], E. Gurpinar Guler[63], C. Isik, O. Kara, A. Kayis Topaksu, U. Kiminsu, G. Onengut, K. Ozdemir[64], A. Polatoz, A. E. Simsek, B. Tali[65], U. G. Tok, S. Turkcapar, I. S. Zorbakir

Physics Department, Middle East Technical University, Ankara, Turkey
G. Karapinar, K. Ocalan[66], M. Yalvac[67]

Bogazici University, Istanbul, Turkey
B. Akgun, I. O. Atakisi, E. Gülmez, M. Kaya[68], O. Kaya[69], Ö. Özçelik, S. Tekten[70], E. A. Yetkin[71]

Istanbul Technical University, Istanbul, Turkey
A. Cakir, K. Cankocak[62], Y. Komurcu, S. Sen[72]

Istanbul University, Istanbul, Turkey
S. Cerci[65], I. Hos[73], B. Isildak[74], B. Kaynak, S. Ozkorucuklu, H. Sert, C. Simsek, D. Sunar Cerci[65], C. Zorbilmez

Institute for Scintillation Materials of National Academy of Science of Ukraine, Kharkiv, Ukraine
B. Grynyov

National Science Centre, Kharkiv Institute of Physics and Technology, Kharkiv, Ukraine
L. Levchuk

University of Bristol, Bristol, UK
D. Anthony, E. Bhal, S. Bologna, J. J. Brooke, A. Bundock, E. Clement, D. Cussans, H. Flacher, J. Goldstein, G. P. Heath, H. F. Heath, L. Kreczko, B. Krikler, S. Paramesvaran, S. Seif El Nasr-Storey, V. J. Smith, N. Stylianou[75], J. Taylor[76], K. Walkingshaw Pass, R. White

Rutherford Appleton Laboratory, Didcot, UK
K. W. Bell, A. Belyaev[77], C. Brew, R. M. Brown, D. J. A. Cockerill, C. Cooke, K. V. Ellis, K. Harder, S. Harper, M.-L. Holmberg, J. Linacre, K. Manolopoulos, D. M. Newbold, E. Olaiya, D. Petyt, T. Reis, T. Schuh, C. H. Shepherd-Themistocleous, I. R. Tomalin, T. Williams

Imperial College, London, UK
R. Bainbridge, P. Bloch, S. Bonomally, J. Borg, S. Breeze, O. Buchmuller, V. Cepaitis, G. S. Chahal[78], D. Colling, P. Dauncey, G. Davies, M. Della Negra, S. Fayer, G. Fedi, G. Hall, M. H. Hassanshahi, G. Iles, J. Langford, L. Lyons, A.-M. Magnan, S. Malik, A. Martelli, D. G. Monk, J. Nash[79], M. Pesaresi,

B. C. Radburn-Smith, D. M. Raymond, A. Richards, A. Rose, E. Scott, C. Seez, A. Shtipliyski, A. Tapper, K. Uchida, T. Virdee[26], M. Vojinovic, N. Wardle, S. N. Webb, D. Winterbottom

Brunel University, Uxbridge, UK
K. Coldham, J. E. Cole, A. Khan, P. Kyberd, I. D. Reid, L. Teodorescu, S. Zahid

Baylor University, Waco, TX, USA
S. Abdullin, A. Brinkerhoff, B. Caraway, J. Dittmann, K. Hatakeyama, A. R. Kanuganti, B. McMaster, N. Pastika, M. Saunders, S. Sawant, C. Sutantawibul, J. Wilson

Catholic University of America, Washington, DC, USA
R. Bartek, A. Dominguez, R. Uniyal, A. M. Vargas Hernandez

The University of Alabama, Tuscaloosa, AL, USA
A. Buccilli, S. I. Cooper, D. Di Croce, S. V. Gleyzer, C. Henderson, C. U. Perez, P. Rumerio[80], C. West

Boston University, Boston, MA, USA
A. Akpinar, A. Albert, D. Arcaro, C. Cosby, Z. Demiragli, E. Fontanesi, D. Gastler, S. May, J. Rohlf, K. Salyer, D. Sperka, D. Spitzbart, I. Suarez, A. Tsatsos, S. Yuan, D. Zou

Brown University, Providence, RI, USA
G. Benelli, B. Burkle, X. Coubez[21], D. Cutts, M. Hadley, U. Heintz, J. M. Hogan[81], T. Kwon, G. Landsberg, K. T. Lau, D. Li, M. Lukasik, J. Luo, M. Narain, N. Pervan, S. Sagir[82], F. Simpson, E. Usai, W. Y. Wong, X. Yan, D. Yu, W. Zhang

University of California, Davis, Davis, CA, USA
J. Bonilla, C. Brainerd, R. Breedon, M. Calderon De La Barca Sanchez, M. Chertok, J. Conway, P. T. Cox, R. Erbacher, G. Haza, F. Jensen, O. Kukral, R. Lander, M. Mulhearn, D. Pellett, B. Regnery, D. Taylor, Y. Yao, F. Zhang

University of California, Los Angeles, CA, USA
M. Bachtis, R. Cousins, A. Datta, D. Hamilton, J. Hauser, M. Ignatenko, M. A. Iqbal, T. Lam, W. A. Nash, S. Regnard, D. Saltzberg, B. Stone, V. Valuev

University of California, Riverside, Riverside, CA, USA
Y. Chen, R. Clare, J. W. Gary, M. Gordon, G. Hanson, G. Karapostoli, O. R. Long, N. Manganelli, W. Si, S. Wimpenny, Y. Zhang

University of California, San Diego, La Jolla, CA, USA
J. G. Branson, P. Chang, S. Cittolin, S. Cooperstein, N. Deelen, D. Diaz, J. Duarte, R. Gerosa, L. Giannini, J. Guiang, R. Kansal, V. Krutelyov, R. Lee, J. Letts, M. Masciovecchio, F. Mokhtar, M. Pieri, B. V. Sathia Narayanan, V. Sharma, M. Tadel, F. Würthwein, Y. Xiang, A. Yagil

Department of Physics, University of California, Santa Barbara, Santa Barbara, CA, USA
N. Amin, C. Campagnari, M. Citron, G. Collura, A. Dorsett, V. Dutta, J. Incandela, M. Kilpatrick, J. Kim, B. Marsh, H. Mei, M. Oshiro, M. Quinnan, J. Richman, U. Sarica, F. Setti, J. Sheplock, P. Siddireddy, D. Stuart, S. Wang

California Institute of Technology, Pasadena, CA, USA
A. Bornheim, O. Cerri, I. Dutta, J. M. Lawhorn, N. Lu, J. Mao, H. B. Newman, T. Q. Nguyen, M. Spiropulu, J. R. Vlimant, C. Wang, S. Xie, Z. Zhang, R. Y. Zhu

Carnegie Mellon University, Pittsburgh, PA, USA
J. Alison, S. An, M. B. Andrews, P. Bryant, T. Ferguson, A. Harilal, C. Liu, T. Mudholkar, M. Paulini, A. Sanchez, W. Terrill

University of Colorado Boulder, Boulder, CO, USA
J. P. Cumalat, W. T. Ford, A. Hassani, G. Karathanasis, E. MacDonald, R. Patel, A. Perloff, C. Savard, N. Schonbeck, K. Stenson, K. A. Ulmer, S. R. Wagner, N. Zipper

Cornell University, Ithaca, NY, USA
J. Alexander, S. Bright-Thonney, X. Chen, Y. Cheng, D. J. Cranshaw, S. Hogan, J. Monroy, J. R. Patterson, D. Quach, J. Reichert, M. Reid, A. Ryd, W. Sun, J. Thom, P. Wittich, R. Zou

Fermi National Accelerator Laboratory, Batavia, IL, USA
M. Albrow, M. Alyari, G. Apollinari, A. Apresyan, A. Apyan, L. A. T. Bauerdick, D. Berry, J. Berryhill, P. C. Bhat, K. Burkett, J. N. Butler, A. Canepa, G. B. Cerati, H. W. K. Cheung, F. Chlebana, K. F. Di Petrillo, J. Dickinson, V. D. Elvira, Y. Feng, J. Freeman, Z. Gecse, L. Gray, D. Green, S. Grünendahl, O. Gutsche, R. M. Harris, R. Heller, T. C. Herwig, J. Hirschauer, B. Jayatilaka, S. Jindariani, M. Johnson, U. Joshi, T. Klijnsma, B. Klima, K. H. M. Kwok, S. Lammel, D. Lincoln, R. Lipton, T. Liu, C. Madrid, K. Maeshima, C. Mantilla, D. Mason, P. McBride, P. Merkel, S. Mrenna, S. Nahn, J. Ngadiuba, V. Papadimitriou, K. Pedro, C. Pena[83], F. Ravera, A. Reinsvold Hall[84], L. Ristori, E. Sexton-Kennedy, N. Smith, A. Soha, L. Spiegel, J. Strait, L. Taylor, S. Tkaczyk, N. V. Tran, L. Uplegger, E. W. Vaandering, H. A. Weber

University of Florida, Gainesville, FL, USA
P. Avery, D. Bourilkov, L. Cadamuro, V. Cherepanov, R. D. Field, D. Guerrero, B. M. Joshi, M. Kim, E. Koenig, J. Konigsberg, A. Korytov, K. H. Lo, K. Matchev, N. Menendez, G. Mitselmakher, A. Muthirakalayil Madhu, N. Rawal, D. Rosenzweig, S. Rosenzweig, K. Shi, J. Wang, Z. Wu, E. Yigitbasi, X. Zuo

Florida State University, Tallahassee, FL, USA
T. Adams, A. Askew, R. Habibullah, V. Hagopian, K. F. Johnson, R. Khurana, T. Kolberg, G. Martinez, H. Prosper, C. Schiber, O. Viazlo, R. Yohay, J. Zhang

Florida Institute of Technology, Melbourne, FL, USA
M. M. Baarmand, S. Butalla, T. Elkafrawy[85], M. Hohlmann, R. Kumar Verma, D. Noonan, M. Rahmani, F. Yumiceva

University of Illinois at Chicago (UIC), Chicago, IL, USA
M. R. Adams, H. Becerril Gonzalez, R. Cavanaugh, S. Dittmer, O. Evdokimov, C. E. Gerber, D. J. Hofman, A. H. Merrit, C. Mills, G. Oh, T. Roy, S. Rudrabhatla, M. B. Tonjes, N. Varelas, J. Viinikainen, X. Wang, Z. Ye

The University of Iowa, Iowa City, IA, USA
M. Alhusseini, K. Dilsiz[86], L. Emediato, R. P. Gandrajula, O. K. Köseyan, J.-P. Merlo, A. Mestvirishvili[87], J. Nachtman, H. Ogul[88], Y. Onel, A. Penzo, C. Snyder, E. Tiras[89]

Johns Hopkins University, Baltimore, MD, USA
O. Amram, B. Blumenfeld, L. Corcodilos, J. Davis, A. V. Gritsan, S. Kyriacou, P. Maksimovic, J. Roskes, M. Swartz, T.Á. Vámi

The University of Kansas, Lawrence, KS, USA
A. Abreu, J. Anguiano, C. Baldenegro Barrera, P. Baringer, A. Bean, Z. Flowers, T. Isidori, S. Khalil, J. King, G. Krintiras, A. Kropivnitskaya, M. Lazarovits, C. Le Mahieu, C. Lindsey, J. Marquez, N. Minafra, M. Murray, M. Nickel, C. Rogan, C. Royon, R. Salvatico, S. Sanders, E. Schmitz, C. Smith, Q. Wang, Z. Warner, J. Williams, G. Wilson

Kansas State University, Manhattan, KS, USA
S. Duric, A. Ivanov, K. Kaadze, D. Kim, Y. Maravin, T. Mitchell, A. Modak, K. Nam

Lawrence Livermore National Laboratory, Livermore, CA, USA
F. Rebassoo, D. Wright

University of Maryland, College Park, MD, USA
E. Adams, A. Baden, O. Baron, A. Belloni, S. C. Eno, N. J. Hadley, S. Jabeen, R. G. Kellogg, T. Koeth, Y. Lai, S. Lascio, A. C. Mignerey, S. Nabili, C. Palmer, M. Seidel, A. Skuja, L. Wang, K. Wong

Massachusetts Institute of Technology, Cambridge, MA, USA
D. Abercrombie, G. Andreassi, R. Bi, W. Busza, I. A. Cali, Y. Chen, M. D'Alfonso, J. Eysermans, C. Freer,

G. Gomez-Ceballos, M. Goncharov, P. Harris, M. Hu, M. Klute, D. Kovalskyi, J. Krupa, Y.-J. Lee, C. Mironov, C. Paus, D. Rankin, C. Roland, G. Roland, Z. Shi, G. S. F. Stephans, J. Wang, Z. Wang, B. Wyslouch

University of Minnesota, Minneapolis, MN, USA
R. M. Chatterjee, A. Evans, J. Hiltbrand, Sh. Jain, M. Krohn, Y. Kubota, J. Mans, M. Revering, R. Rusack, R. Saradhy, N. Schroeder, N. Strobbe, M. A. Wadud

University of Nebraska-Lincoln, Lincoln, NE, USA
K. Bloom, M. Bryson, S. Chauhan, D. R. Claes, C. Fangmeier, L. Finco, F. Golf, C. Joo, I. Kravchenko, I. Reed, J. E. Siado, G. R. Snow[†], W. Tabb, A. Wightman, F. Yan, A. G. Zecchinelli

State University of New York at Buffalo, Buffalo, NY, USA
G. Agarwal, H. Bandyopadhyay, L. Hay, I. Iashvili, A. Kharchilava, C. McLean, D. Nguyen, J. Pekkanen, S. Rappoccio, A. Williams

Northeastern University, Boston, MA, USA
G. Alverson, E. Barberis, Y. Haddad, Y. Han, A. Hortiangtham, A. Krishna, J. Li, J. Lidrych, G. Madigan, B. Marzocchi, D. M. Morse, V. Nguyen, T. Orimoto, A. Parker, L. Skinnari, A. Tishelman-Charny, T. Wamorkar, B. Wang, A. Wisecarver, D. Wood

Northwestern University, Evanston, IL, USA
S. Bhattacharya, J. Bueghly, Z. Chen, A. Gilbert, T. Gunter, K. A. Hahn, Y. Liu, N. Odell, M. H. Schmitt, M. Velasco

University of Notre Dame, Notre Dame, IN, USA
R. Band, R. Bucci, M. Cremonesi, A. Das, N. Dev, R. Goldouzian, M. Hildreth, K. Hurtado Anampa, C. Jessop, K. Lannon, J. Lawrence, N. Loukas, L. Lutton, J. Mariano, N. Marinelli, I. Mcalister, T. McCauley, C. Mcgrady, K. Mohrman, C. Moore, Y. Musienko[13], R. Ruchti, A. Townsend, M. Wayne, M. Zarucki, L. Zygala

The Ohio State University, Columbus, OH, USA
B. Bylsma, L. S. Durkin, B. Francis, C. Hill, M. Nunez Ornelas, K. Wei, B. L. Winer, B. R. Yates

Princeton University, Princeton, NJ, USA
F. M. Addesa, B. Bonham, P. Das, G. Dezoort, P. Elmer, A. Frankenthal, B. Greenberg, N. Haubrich, S. Higginbotham, A. Kalogeropoulos, G. Kopp, S. Kwan, D. Lange, D. Marlow, K. Mei, I. Ojalvo, J. Olsen, D. Stickland, C. Tully

University of Puerto Rico, Mayaguez, PR, USA
S. Malik, S. Norberg

Purdue University, West Lafayette, IN, USA
A. S. Bakshi, V. E. Barnes, R. Chawla, S. Das, L. Gutay, M. Jones, A. W. Jung, D. Kondratyev, A. M. Koshy, M. Liu, G. Negro, N. Neumeister, G. Paspalaki, S. Piperov, A. Purohit, J. F. Schulte, M. Stojanovic, J. Thieman, F. Wang, R. Xiao, W. Xie

Purdue University Northwest, Hammond, IN, USA
J. Dolen, N. Parashar

Rice University, Houston, TX, USA
D. Acosta, A. Baty, T. Carnahan, M. Decaro, S. Dildick, K. M. Ecklund, S. Freed, P. Gardner, F. J. M. Geurts, A. Kumar, W. Li, B. P. Padley, R. Redjimi, J. Rotter, W. Shi, A. G. Stahl Leiton, S. Yang, L. Zhang[90], Y. Zhang

University of Rochester, Rochester, NY, USA
A. Bodek, P. de Barbaro, R. Demina, J. L. Dulemba, C. Fallon, T. Ferbel, M. Galanti, A. Garcia-Bellido, O. Hindrichs, A. Khukhunaishvili, E. Ranken, R. Taus, G. P. Van Onsem

Rutgers, The State University of New Jersey, Piscataway, NJ, USA
B. Chiarito, J. P. Chou, A. Gandrakota, Y. Gershtein, E. Halkiadakis, A. Hart, M. Heindl, O. Karacheban[24], I. Laflotte, A. Lath, R. Montalvo, K. Nash, M. Osherson, S. Salur, S. Schnetzer, S. Somalwar, R. Stone, S. A. Thayil, S. Thomas, H. Wang

University of Tennessee, Knoxville, TN, USA
H. Acharya, A. G. Delannoy, S. Fiorendi, S. Spanier

Texas A&M University, College Station, TX, USA
O. Bouhali[91], M. Dalchenko, A. Delgado, R. Eusebi, J. Gilmore, T. Huang, T. Kamon[92], H. Kim, S. Luo, S. Malhotra, R. Mueller, D. Overton, D. Rathjens, A. Safonov

Texas Tech University, Lubbock, TX, USA
N. Akchurin, J. Damgov, V. Hegde, S. Kunori, K. Lamichhane, S. W. Lee, T. Mengke, S. Muthumuni, T. Peltola, I. Volobouev, Z. Wang, A. Whitbeck

Vanderbilt University, Nashville, TN, USA
E. Appelt, S. Greene, A. Gurrola, W. Johns, A. Melo, K. Padeken, F. Romeo, P. Sheldon, S. Tuo, J. Velkovska

University of Virginia, Charlottesville, VA, USA
M. W. Arenton, B. Cardwell, B. Cox, G. Cummings, J. Hakala, R. Hirosky, M. Joyce, A. Ledovskoy, A. Li, C. Neu, C. E. Perez Lara, B. Tannenwald, S. White

Wayne State University, Detroit, MI, USA
N. Poudyal

University of Wisconsin-Madison, Madison, WI, USA
S. Banerjee, K. Black, T. Bose, S. Dasu, I. De Bruyn, P. Everaerts, C. Galloni, H. He, M. Herndon, A. Herve, U. Hussain, A. Lanaro, A. Loeliger, R. Loveless, J. Madhusudanan Sreekala, A. Mallampalli, A. Mohammadi, D. Pinna, A. Savin, V. Shang, V. Sharma, W. H. Smith, D. Teague, S. Trembath-Reichert, W. Vetens

Authors affiliated with an Institute or an international laboratory covered by a cooperation agreement with CERN, Geneva, Switzerland
S. Afanasiev, V. Andreev, Yu. Andreev, T. Aushev, M. Azarkin, A. Babaev, A. Belyaev, V. Blinov[93], E. Boos, V. Borshch, D. Budkouski, V. Bunichev, O. Bychkova, V. Chekhovsky, R. Chistov[93], M. Danilov[93], A. Dermenev, T. Dimova[93], I. Dremin, M. Dubinin[83], L. Dudko, V. Epshteyn[94], G. Gavrilov, V. Gavrilov, S. Gninenko, V. Golovtcov, N. Golubev, I. Golutvin, I. Gorbunov, A. Gribushin, V. Ivanchenko, Y. Ivanov, V. Kachanov, L. Kardapoltsev[93], V. Karjavine, A. Karneyeu, V. Kim[93], M. Kirakosyan, D. Kirpichnikov, M. Kirsanov, V. Klyukhin, O. Kodolova[95], D. Konstantinov, V. Korenkov, A. Kozyrev[93], N. Krasnikov, E. Kuznetsova[96], A. Lanev, A. Litomin, N. Lychkovskaya, V. Makarenko, A. Malakhov, V. Matveev[93], V. Murzin, A. Nikitenko[97], S. Obraztsov, V. Okhotnikov, V. Oreshkin, A. Oskin, I. Ovtin[93], V. Palichik, P. Parygin[98], A. Pashenkov, V. Perelygin, M. Perfilov, S. Petrushanko, G. Pivovarov, S. Polikarpov[93], V. Popov, O. Radchenko[93], M. Savina, V. Savrin, V. Shalaev, S. Shmatov, S. Shulha, Y. Skovpen[93], S. Slabospitskii, I. Smirnov, V. Smirnov, D. Sosnov, A. Stepennov, V. Sulimov, E. Tcherniaev, A. Terkulov, O. Teryaev, M. Toms[99], A. Toropin, L. Uvarov, A. Uzunian, E. Vlasov[100], S. Volkov, A. Vorobyev, N. Voytishin, B. S. Yuldashev[101], A. Zarubin, I. Zhizhin, A. Zhokin

† **Deceased**

1: Also at Yerevan State University, Yerevan, Armenia
2: Also at TU Wien, Vienna, Austria
3: Also at Institute of Basic and Applied Sciences, Faculty of Engineering, Arab Academy for Science, Technology and Maritime Transport, Alexandria, Egypt
4: Also at Université Libre de Bruxelles, Brussels, Belgium
5: Also at Universidade Estadual de Campinas, Campinas, Brazil
6: Also at Federal University of Rio Grande do Sul, Porto Alegre, Brazil

7: Also at The University of the State of Amazonas, Manaus, Brazil
8: Also at University of Chinese Academy of Sciences, Beijing, China
9: Also at UFMS, Nova Andradina, Brazil
10: Also at Nanjing Normal University Department of Physics, Nanjing, China
11: Now at The University of Iowa, Iowa City, IA, USA
12: Also at University of Chinese Academy of Sciences, Beijing, China
13: Also at an institute or an international laboratory covered by a cooperation agreement with CERN, Geneva, Switzerland
14: Also at Helwan University, Cairo, Egypt
15: Now at Zewail City of Science and Technology, Zewail, Egypt
16: Now at British University in Egypt, Cairo, Egypt
17: Also at Purdue University, West Lafayette, IN, USA
18: Also at Université de Haute Alsace, Mulhouse, France
19: Also at Ilia State University, Tbilisi, Georgia
20: Also at Erzincan Binali Yildirim University, Erzincan, Turkey
21: Also at RWTH Aachen University, III. Physikalisches Institut A, Aachen, Germany
22: Also at University of Hamburg, Hamburg, Germany
23: Also at Isfahan University of Technology, Isfahan, Iran
24: Also at Brandenburg University of Technology, Cottbus, Germany
25: Also at Forschungszentrum Jülich, Jülich, Germany
26: Also at CERN, European Organization for Nuclear Research, Geneva, Switzerland
27: Also at Physics Department, Faculty of Science, Assiut University, Assiut, Egypt
28: Also at Karoly Robert Campus, MATE Institute of Technology, Gyongyos, Hungary
29: Also at Institute of Physics, University of Debrecen, Debrecen, Hungary
30: Also at Institute of Nuclear Research ATOMKI, Debrecen, Hungary
31: Now at Universitatea Babes-Bolyai-Facultatea de Fizica, Cluj-Napoca, Romania
32: Also at MTA-ELTE Lendület CMS Particle and Nuclear Physics Group, Eötvös Loránd University, Budapest, Hungary
33: Also at Wigner Research Centre for Physics, Budapest, Hungary
34: Also at Punjab Agricultural University, Ludhiana, India
35: Also at UPES-University of Petroleum and Energy Studies, Dehradun, India
36: Also at Shoolini University, Solan, India
37: Also at University of Hyderabad, Hyderabad, India
38: Also at University of Visva-Bharati, Santiniketan, India
39: Also at Indian Institute of Science (IISc), Bangalore, India
40: Also at Indian Institute of Technology (IIT), Mumbai, India
41: Also at IIT Bhubaneswar, Bhubaneswar, India
42: Also at Institute of Physics, Bhubaneswar, India
43: Also at Deutsches Elektronen-Synchrotron, Hamburg, Germany
44: Also at Sharif University of Technology, Tehran, Iran
45: Also at Department of Physics, University of Science and Technology of Mazandaran, Behshahr, Iran
46: Also at Italian National Agency for New Technologies, Energy and Sustainable Economic Development, Bologna, Italy
47: Also at Centro Siciliano di Fisica Nucleare e di Struttura Della Materia, Catania, Italy
48: Also at Scuola Superiore Meridionale, Università di Napoli 'Federico II', Naples, Italy
49: Also at Università di Napoli 'Federico II', Naples, Italy
50: Also at Consiglio Nazionale delle Ricerche-Istituto Officina dei Materiali, Perugia, Italy
51: Also at Consejo Nacional de Ciencia y Tecnología, Mexico City, Mexico
52: Also at IRFU, CEA, Université Paris-Saclay, Gif-sur-Yvette, France
53: Also at Faculty of Physics, University of Belgrade, Belgrade, Serbia
54: Also at Trincomalee Campus, Eastern University, Nilaveli, Sri Lanka
55: Also at INFN Sezione di Pavia, Università di Pavia, Pavia, Italy
56: Also at National and Kapodistrian University of Athens, Athens, Greece
57: Also at Ecole Polytechnique Fédérale Lausanne, Lausanne, Switzerland
58: Also at Universität Zürich, Zurich, Switzerland
59: Also at Stefan Meyer Institute for Subatomic Physics, Vienna, Austria

60: Also at Laboratoire d'Annecy-le-Vieux de Physique des Particules, IN2P3-CNRS, Annecy-le-Vieux, France
61: Also at Şırnak University, Sirnak, Turkey
62: Also at Near East University, Research Center of Experimental Health Science, Mersin, Turkey
63: Also at Konya Technical University, Konya, Turkey
64: Also at Izmir Bakircay University, Izmir, Turkey
65: Also at Adiyaman University, Adiyaman, Turkey
66: Also at Necmettin Erbakan University, Konya, Turkey
67: Also at Bozok Universitetesi Rektörlügü, Yozgat, Turkey
68: Also at Marmara University, Istanbul, Turkey
69: Also at Milli Savunma University, Istanbul, Turkey
70: Also at Kafkas University, Kars, Turkey
71: Also at Istanbul Bilgi University, Istanbul, Turkey
72: Also at Hacettepe University, Ankara, Turkey
73: Also at Istanbul University-Cerrahpasa, Faculty of Engineering, Istanbul, Turkey
74: Also at Ozyegin University, Istanbul, Turkey
75: Also at Vrije Universiteit Brussel, Brussels, Belgium
76: Also at Rutherford Appleton Laboratory, Didcot, UK
77: Also at School of Physics and Astronomy, University of Southampton, Southampton, UK
78: Also at IPPP Durham University, Durham, UK
79: Faculty of Science, Also at Monash University, Clayton, Australia
80: Also at Università di Torino, Turin, Italy
81: Also at Bethel University, St. Paul, MN, USA
82: Also at Karamanoğlu Mehmetbey University, Karaman, Turkey
83: Also at California Institute of Technology, Pasadena, CA, USA
84: Also at United States Naval Academy, Annapolis, MD, USA
85: Also at Ain Shams University, Cairo, Egypt
86: Also at Bingol University, Bingol, Turkey
87: Also at Georgian Technical University, Tbilisi, Georgia
88: Also at Sinop University, Sinop, Turkey
89: Also at Erciyes University, Kayseri, Turkey
90: Also at Institute of Modern Physics and Key Laboratory of Nuclear Physics and Ion-beam Application (MOE), Fudan University, Shanghai, China
91: Also at Texas A&M University at Qatar, Doha, Qatar
92: Also at Kyungpook National University, Daegu, Korea
93: Also at another institute or international laboratory covered by a cooperation agreement with CERN, Geneva, Switzerland
94: Now at Istanbul University, Istanbul, Turkey
95: Also at Yerevan Physics Institute, Yerevan, Armenia
96: Also at University of Florida, Gainesville, FL, USA
97: Also at Imperial College, London, UK
98: Now at University of Rochester, Rochester, NY, USA
99: Now at Baylor University, Waco, TX, USA
100: Now at INFN Sezione di Torino, Università di Torino, Turin, Italy, Università del Piemonte Orientale, Novara, Italy
101: Also at Institute of Nuclear Physics of the Uzbekistan Academy of Sciences, Tashkent, Uzbekistan